A comprehensive transcriptome analysis of silique development and dehiscence in Arabidopsis and Brassica integrating genotypic, interspecies and developmental comparisons

Jaradat, Masrur R.; Ruegger, Max; Bowling, Andrew; Butler, Holly; Cutler, Adrian J.

Publisher's version / Version de l'éditeur:
https://doi.org/10.4161/21645698.2014.947827
GM Crops & Food, 5, 4, pp. 302-320, 2014-10-30

RESEARCH PAPER

GM Crops & Food 5:4, 302–320; October/November/December 2014; © 2014 National Research Council of Canada

A comprehensive transcriptome analysis of silique development and dehiscence in *Arabidopsis* and *Brassica* integrating genotypic, interspecies and developmental comparisons

Masrur R Jaradat[1], Max Ruegger[2], Andrew Bowling[2], Holly Butler[2], and Adrian J Cutler[1,*]

[1]National Research Council of Canada; Saskatoon, Canada; [2]Dow AgroSciences LLC; Indianapolis, IN USA

Keywords: *Arabidopsis thaliana*, *Brassica juncea*, *Brassica napus*, microarray, mutants, pod shatter, silique dehiscence

Abbreviations: DZ, dehiscence zone; En*b*, endocarp *b;* LL, lignified layer; SL, separation layer; SSP, seed storage protein; TF, transcription factor; VM, valve margin; WT, wild type

Asynchronous flowering of *Brassica napus* (canola) leads to seeds and siliques at varying stages of maturity as harvest approaches. This range of maturation can result in premature silique dehiscence (pod shattering), resulting in yield losses, which may be worsened by environmental stresses. Therefore, a goal for canola crop improvement is to reduce shattering in order to maximize yield. We performed a comprehensive transcriptome analysis on the dehiscence zone (DZ) and valve of *Arabidopsis* and *Brassica* siliques in shatter resistant and sensitive genotypes at several developmental stages. Among known *Arabidopsis* dehiscence genes, we confirmed that homologs of *SHP1/2*, *FUL*, *ADPG1*, *NST1/3* and *IND* were associated with shattering in *B. juncea* and *B. napus*. We noted a correlation between reduced pectin degradation genes and shatter-resistance. Tension between lignified and non-lignified cells in the silique DZ plays a major role in dehiscence. Light microscopy revealed a smaller non-lignified separation layer in relatively shatter-resistant *B. juncea* relative to *B. napus* and this corresponded to increased expression of peroxidases involved in monolignol polymerization. Sustained repression of auxin biosynthesis, transport and signaling in *B. juncea* relative to *B. napus* may cause differences in dehiscence zone structure and cell wall constituents. Tension on the dehiscence zone is a consequence of shrinkage and loss of flexibility in the valves, which is caused by senescence and desiccation. Reduced shattering was generally associated with upregulation of ABA signaling and down-regulation of ethylene and jasmonate signaling, corresponding to more pronounced stress responses and reduced senescence and photosynthesis. Overall, we identified 124 cell wall related genes and 103 transcription factors potentially involved in silique dehiscence.

Introduction

Canola is an economically successful oil crop because of its healthy fatty acid composition and high yield. However, the precise timing of crop harvest is challenging due to non-uniform seed maturity caused by asynchronous flowering. On the one hand, premature harvest results in poor oil quality due to the relatively high moisture and chlorophyll content of immature seeds. On the other hand, late harvesting results in yield losses of 8%-12%, and up to 50% under extreme conditions, since fully mature canola siliques are extremely sensitive to premature dehiscence, referred to as pod shatter.[1,2,3] The timing challenge for harvest is exacerbated by water, wind and heat stresses; each of which can increase dehiscence. Attempts have been made to increase shatter resistance through conventional breeding since genetic variation for shattering occurs in the *Brassica* family. For example, *B. juncea* is relatively shatter resistant compared to canola.[2] However, traditional breeding methods have so far been unsuccessful. Reduction of shattering has been accomplished in *Arabidopsis* by transgenic manipulation of upstream regulatory transcription factors (TFs) such as *SHATTERPROOF1* and 2 (*SHP1/2*), *FRUITFULL* (*FUL*), *ALCATRAZ* (*ALC*) and *INDEHISCENT* (*IND*) as well as with downstream TFs or metabolic genes.[4-8] However, the goal of reducing premature shattering while simultaneously maintaining facile seed release at maturity has proved challenging.

Dry fruit (capsule) development and subsequent dehiscence is a complex and highly organized process. The progressive development of fruits is coordinated with that of enclosed seeds and climaxes with capsule dehiscence (shattering) allowing seed dispersal. Crucifer capsules consist of 2 fused carpels divided by a false septum and are termed siliques. The fused carpels develop into valves that are joined with 2 medial repla which border the septum; seeds are attached to the septum by funicles. The valve and replum are separated by the valve margin (VM) consisting of

*Correspondence to: Adrian J Cutler; Email: Adrian.cutler@nrc-cnrc.gc.ca
Submitted: 01/22/2014; Revised: 05/07/2014; Accepted: 05/14/2014
http://dx.doi.org/10.4161/21645698.2014.947827

cells that differentiate to become the dehiscence zone (DZ). The valves separate at the DZ during pod shattering. Development of *Arabidopsis thaliana* siliques has been studied extensively (for reviews see refs. 9, 10).

There are 2 cell types in the DZ. One type constitutes the non-lignified separation layer (SL) which is juxtaposed with the replum and allows the detachment of valves via cell-cell separation.[11] The other VM cells are remote from the replum and form a rigid lignified layer (LL) which is continuous with the lignified endocarp *b* (en*b*) of the valve.[12,13]

The *INDEHISCENT* (*IND*) TF is responsible for the differentiation of the VM into the LL and SL by regulation of auxin transport[14] whereas the TF *ALCATRAZ* (*ALC*) regulates the development of the SL.[5,15] Lignification in the valve is controlled by *IND* and *ALC*, as well as *SHP1*, *SHP2* and *FUL*.[5] It has been postulated that during capsule desiccation tension builds up between rigid lignified and non-lignified layers to potentiate valve detachment.[16] *SHP1/2* promotes lignification of VM adjacent to the DZ. In the double mutant *shp1/2*, DZ formation and lignin deposition in the VM do not occur resulting in indehiscent siliques. *FUL* promotes valve differentiation and expansion (suppressing *SHP* and *IND* activity) and prevents VM lignification.[5,17,18] Consequently, *ful* siliques are 80% smaller than WT siliques and there is ectopic lignification of all internal valve mesophyll cells and reduced shattering relative to WT. The association of reduced shattering and ectopic lignification in *ful* may be due to elimination of the tension between lignified and non-lignified cells. On the other hand, in siliques over-expressing *FUL*, both VM and replum cells become valve-like with no DZ or lignification resulting in completely indehiscent siliques.[18] Siliques of *alc* acquire ectopically lignified cells in the inner VM that forms a continuous lignified bridge between lignified inner valve cell layers and the lignified replum vasculature and are indehiscent.[15] Replum identity is specified by *REPLUMLESS* (*RPL*), which represses *SHP1/2*.[10]

After establishment of tissue identity, secondary wall deposition occurs in cells adjacent to the SL and in the valve endocarp. This deposition is required for dehiscence and is positively regulated by 2 plant-specific TFs *NAC SECONDARY WALL THICKENING PROMOTING FACTOR* 1 and 3 (*NST1* and *NST3*) in a partially redundant manner and loss of function mutants of *NST1/3* are indehiscent.[7]

A growing body of evidences supports the long-held hypothesis that the degradation of middle lamella and cell wall in the SL loosens cellular cohesion leading to valve detachment and that this engages proteins involved in cell wall loosening and hydrolysis such as cellulase (β-1,4 glucanase,), polygalacturonase (PG) and expansin.[11,19-23] Direct evidence for this hypothesis came from studies on loss-of-function mutants of 2 closely related endo-PGs, *ARABIDOPSIS DZ POLYGALACTURONASE1* (*ADPG1*) and *ADPG2*, which resulted in indehiscent siliques.[8] *ADPG1/2* act in a partially redundant fashion and normal expression of *ADPG1* in the silique DZ depends on *IND*.

However, other factors in addition to cell wall composition may influence shattering. Magnetic resonance imaging of silique desiccation revealed that shatter sensitive *B. napus* (cv. Quantum) lost water from the inside of the valve in contrast with shatter resistant *B. rapa* (cv Parkland) which lost water from the outside of the valve.[24] This suggested that the pattern of water loss contributed to a difference in tension on the SL and hence to a difference in susceptibility to shatter between the 2 cultivars.

A link between pod shatter TFs and hormonal regulation was revealed by the discovery that *IND* modulates auxin distribution by relocating the auxin efflux carrier *PIN FORMED1* (*PIN1*) in the SL cells as they differentiate.[14] In addition *IND* causes localized GA production leading to de-repression of *ALC* by DELLA proteins and hence (as noted earlier) to SL development.[25] Reduced ethylene production in parthenocarpic (seedless) pods of canola was correlated with delayed pod dehiscence which was restored by application of the ethylene releasing chemical ethephon.[26] On the other hand, siliques of loss-of-function mutants of ethylene receptors in *Arabidopsis* shatter at the normal time.[26] Ethylene production was studied in shatter resistant *B. juncea* (mustard) and shatter sensitive canola and was very low in silique wall and high in seeds in both species.[27,27] Interestingly, there was considerably higher ethylene inside mustard siliques than inside canola siliques and this interspecies difference became larger toward desiccation.[27]

The process of pod dehiscence in *Arabidopsis* is similar to that in canola based on comparative anatomical and physiological studies.[16] Although several groups have identified regulators and metabolic genes involved in silique dehiscence that are described above, a complete description of shatter-related processes has not yet been obtained. In this paper, we present a comprehensive transcriptome analysis using: (1) shatter resistant and –sensitive *Arabidopsis* and *Brassica* genotypes and (2) selected developmental stages to identify genes that are differentially regulated between genotypes differing in shattering. Integration of transcriptome data from genotypic, interspecies and developmental comparisons has uncovered genes whose functions and pattern of expression suggest roles in pod development and dehiscence.

Results

Experimental design

The Combimatrix 90k Brassica array covers about 64% of the corresponding genes in the *Arabidopsis* genome and 78% of the ~90000 contigs represented on the array were aligned with *Arabidopsis* genes. About 80% of *Arabidopsis* genes on the array corresponded to multiple *Brassica* probes (contigs).[28] The effect of multiple probes for most *Arabidopsis* genes was to increase replication and hence the reliability of the *Brassica* transcriptome analysis. *Arabidopsis* microarray hybridizations (2 color) were performed between whole siliques of each of the shatter mutants – *shp1xshp2*, *ful*, and *alc* with that of WT and between manually peeled valve of *B. juncea* and *B. napus* at 3 developmental stages (3, 5 and 6) as described in the methods section (**Table 1**). Since *Arabidopsis* and *Brassica* share 86% DNA homology in protein coding regions, we initially hybridized *Brassica* onto *Arabidopsis* arrays. Such heterologous probing has been successfully employed in previous studies (e.g. see ref. 29). We later used homologous probing to the Brassica Combimatrix arrays described above.

Table 1. Experiments and number of probed arrays used for data analysis

Experiment I (*Arabidopsis* whole siliques; mutant vs. WT; Two color; *Arabidopsis* full genome oligo arrays)

Genotype	stage 3	stage 5	stage 6
shp1xshp2 vs. WT	6	6	6
alc vs. WT	6	6	6
ful vs. WT	6	6	6

Experiment II (*Brassica* tissues; 2 color; *Arabidopsis* full genome oligo arrays)

Genotype	stage 2	stage 3	stage 5	stage 6
DZ: *B. juncea* vs. *B. napus*	2	—	—	—
Valve: *B. juncea* vs. *B. napus*	2	4	5	6

Experiment III (*Arabidopsis* pod; 2 color; *Arabidopsis* full genome oligo arrays)

Genotype	6 DPA	11 DPA	14 DPA
ful vs. WT	4	4	4

Experiment IV (*Brassica* tissues; single color; Combimatrix 90k *Brassica* oligo arrays)

Genotype	stage 1	stage 2	stage 4	stage 5	stage 6
B. juncea DZ	6	6	6	—	—
B. juncea valve	6	6	6	5	6
B. napus DZ	5	6	5	—	—
B. napus valve	6	6	5	4	4

Numbers indicate probed arrays used for data analysis and obtained after quality control on samples in GeneSpring.

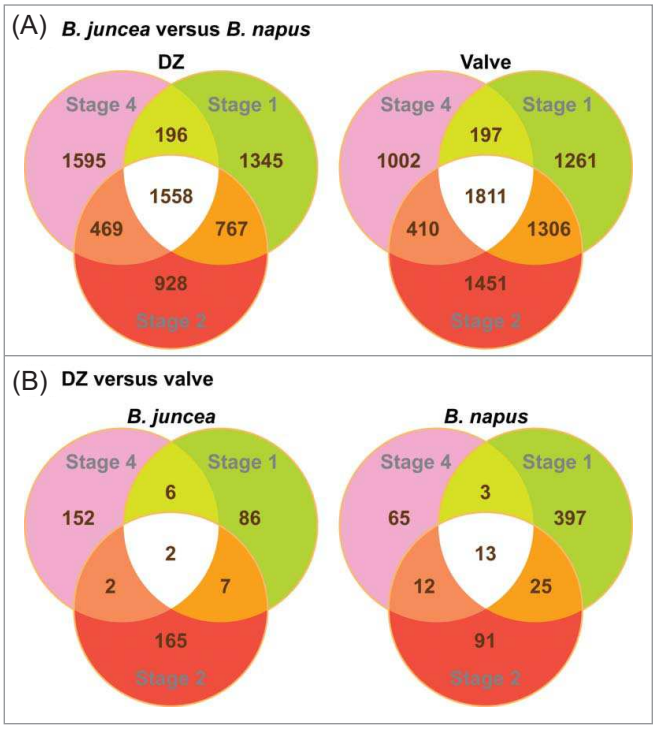

Figure 1. Venn diagrams to illustrate differences in transcript profiles of *Brassica* tissues between genotypes and at various stages.

First, we compared the expression of known shatter-related genes such as *ADPG1* in our microarray data with published results. Promoter-*GUS* analysis clearly demonstrated that *ADPG1* is expressed in DZ but not in valve.[8] In contrast, we detected moderate to high expression of *ADPG1* in manually dissected valves. We concluded that valves contained residual DZ. In order to improve tissue uniformity and to explore gene expression at earlier stages, we dissected DZ and valve of *B. napus* and *B. juncea* microscopically at stages 1, 2 and 4 for definitive expression studies (**Table 1**). There were substantial differences in transcript profiles between *B. juncea* and *B. napus* as reflected by the high number of differentially expressed genes in both DZ and valve (**Fig. 1A; Figs. S2A, S3**). In contrast, there were fewer differences between the transcript profiles of DZ and valve within the same *Brassica* species (**Fig. 1B**). Therefore, we concluded that the effect of residual DZ on gene expression changes in manually dissected *Brassica* valve would be negligible. Consequently, we analyzed microarray data from all dissected *Brassica* tissues and *Brassica* analysis below refers to both experiments. In addition, a second set of gene expression comparisons in *Arabidopsis* pod tissues (with seeds removed for greater specificity) between *ful* and WT at earlier stages including 6 days post anthesis (DPA), 11 DPA and 14 DPA were performed. Since *FUL* is a negative regulator of dehiscence, genes associated with shattering will be overexpressed in valves in the *ful* background. Most of the *Arabidopsis* analyses refer to these second set of experiments.

Comparing *Arabidopsis* shatter mutants

The number of expressed genes as a percentage of the full *Arabidopsis* genome was calculated for each class of experiments. This percentage was 20 ± 2.6% for initial *Arabidopsis* comparisons and 74.7 ± 3.8% for *Arabidopsis* comparisons of *ful* vs. WT using the more sensitive RNA amplification protocol with seeds removed. The relatively low number of significantly expressed genes in whole siliques of *Arabidopsis* mutant versus WT comparisons (**Table 2**) could be partly due to the presence of highly abundant transcripts associated with seed nutrient reserve accumulation that may dilute out less abundant silique transcripts.

Genes encoding seed storage proteins

Accumulation of nutrient reserves during *Arabidopsis* and *Brassica* seed and *Arabidopsis* silique development has been extensively documented.[30,31] Different classes of seed storage proteins (SSPs) accumulate at the mid maturation stage of seed development but follow distinct temporal expression patterns.[30]

Table 2. Number of significantly up- and downregulated genes (indicated by arrows) using a threshold change in expression of 1.5 fold and a *p*-value cut-off: ≤0.05

	Whole silique			
	***shp1 xshp2* vs. Col-0**	***alc* vs. Col-0**	***ful* vs. Col-0**	**Pod *ful* vs. Col-0**
Stage 3	189↑; 86↓	24↑; 233↓	28↑; 10↓	—
Stage 5	55↑; 146↓	35↑; 94↓	157↑; 230↓	—
Stage 6	78↑; 65↓	0↑; 56↓	60↑; 14↓	v
6 DPA	—	—	—	479↑; 778↓
11 DPA	—	—	—	576↑; 876↓
14 DPA	—	—	—	245↑; 294↓

Interestingly, SSP genes were the most highly upregulated genes in *Arabidopsis* pod starting from a very low level at 10 DPA but increasing almost 500 fold by 20 DPA.[31] The expression of nutrient reserve transcripts including cruciferin, napin, oleosin, and late embryogenesis-associated (LEA) proteins in DZ of both *B. juncea* and *B. napus*, were highly upregulated at stage 4 (green-yellow tissue) with expression up to 170 fold above the basal level in *B. juncea* compared to 14-fold in *B. napus* (**Fig. 2A; Table S3**). The upregulation of storage product transcripts occurred at stage 2 of *B. juncea* valve. Accumulation of storage product transcripts in *B. napus* valve and DZ was very similar. Oddly enough, after a decline at stages 4 and 5, the transcripts were upregulated at stage 6 in valves of *B. juncea*.

In the *Arabidopsis ful* vs. WT (**Fig. 2B; Table S3**), the expression of SSPs was downregulated at 6 DPA but upregulated in 11 DPA and 14 DPA which indicates a possible role of *FUL* in regulating expression of storage proteins.

ABI3, *FUS3*, *LEC1* and *LEC2* are master regulators of SSP accumulation in seeds.[32] However, we were unable to detect *LEC2* and *ABI3* transcripts in pods of *Arabidopsis* and *Brassica*. *FUS3* and *LEC1* were expressed in pods at very low levels and were not differentially expressed in *ful* vs. WT and *B. juncea* vs. *B. napus* comparisons. We performed SOM clustering among these nutrient reserve genes and differentially expressed significant TFs (fold change ≥4 and p-value cutoff ≤0.05) and identified 3 NAC TFs whose transcript profiles preceded those of the SSP transcripts (**Fig. 2C**). These TFs, *NAC010* (At1g28470 [2 contigs]), *NAC036* (At2g17040 [3 contigs]) and NAC073 (At4g28500 [2 contigs]), may be involved in the regulation of seed storage product accumulation in siliques.

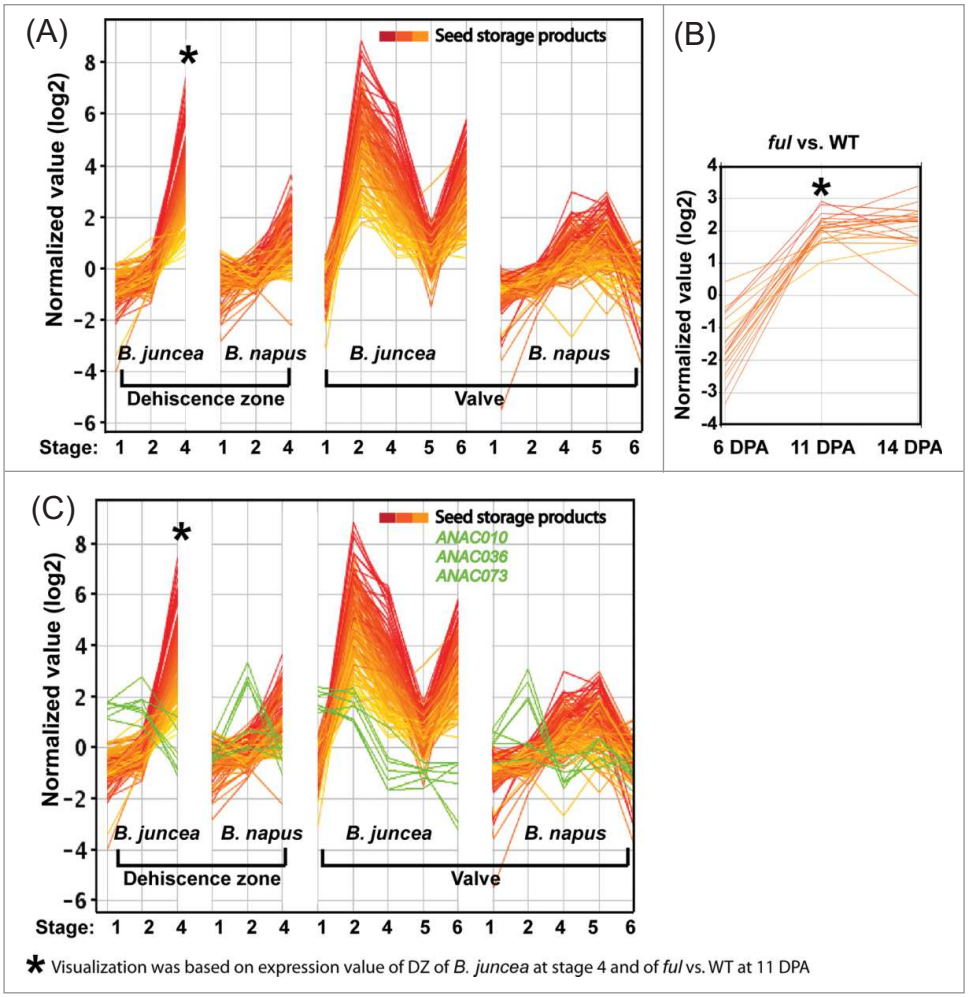

Figure 2. Comparison of transcript profiles of genes related to nutrient reserves between *B. juncea* and *B. napus* and between *Arabidopsis ful* and WT. Expression of individual contigs associated with *Arabidopsis* nutrient reserve was measured in various tissues of *B. juncea* and *B. napus* at different developmental stages using *Brassica* (Combimatrix, single color) microarray hybridization **(A), (C)**. Expression of sequences corresponding to 3 Arabidopsis NAC TFs are overlaid on the SSP data in green (**C**). Expression profiles of nutrient reserve genes were compared in pod tissues of *Arabidopsis ful* vs. WT using *Arabidopsis* microarray (oligonucleotide probes, 2 color) hybridization **(B)**.

The expression of known dehiscence genes

The Combimatrix microarray contained probes corresponding to *SHP*1, *SHP2*, *FUL*, *ALC*, *ADPG2* and *NST3*, but none for *IND*, *NST1*, *NST2* and *ADPG1*. Expression of both *SHP1/2* genes showed similar profiles (**Fig. 3A**) and interestingly were higher in DZ than in valve at stages 1 and 2 in both *B. juncea* and *B. napus*. In contrast, the expression of *FUL* was lower in DZ than in valve at stages 1 and 2 of both *Brassica* cultivars. The expression of *SHP1/2* were much higher than *FUL* in DZ of *B. napus* but the expression levels of these 3 TFs were similar in DZ of *B. juncea*. This is consistent with the fact that pods of *B. napus* are more shatter sensitive than *B. juncea* since we might expect expression of positive shatter regulators such as *SHP1* and *SHP2* to be relatively high, whereas expression of negative regulator *FUL* to be relatively low in DZ of siliques nearing dehiscence.

Intriguingly, the *SHP1/2* expression levels in manually dissected valve at stages 5 and 6 (**Fig. 3A**), were higher in *B. juncea* than in *B. napus* and were verified by 2 color direct comparisons (**Table S1**).

FUL expression in DZ and valve at all stages studied was consistently 1.5-2 fold higher in *B. juncea* than in *B. napus* (**Fig. 3A**). The expression profile of *ALC* was opposite to that of *SHP1/2* in DZ at stage 3

and in valve at all stages studied of both *Brassica* cultivars (**Fig. 3A**). Using heterologous *Arabidopsis* oligo arrays, no or low signal was detected for *ALC, ADPG2*, *IND* and *NST2* (signal intensity of 200 for *ALC* and *ADPG2* using RNA amplification system) in *Brassica* valves. It has been shown previously that *FUL* represses the expression of *SHP1/2*, *IND* and *ALC*.[5,18] *IND* activates the expression of *ADPG1* in the silique DZ.[8]

Dehiscence genes that were upregulated in pods of *ful* plants compared to that of WT included *IND* (12.93 fold), *ADPG2* (11.08 fold), *ADPG1* (4.95 fold), *FIL* (4.27 fold), *SHP1* (3.26 fold), *PID* (3.13 fold), and *SHP2* (2.72 fold) (**Table 3**). Indeed, in pods of *ful*, expression of all the positive regulators of dehiscence except *ALC* were upregulated compared to WT and therefore consistent with the role of *FUL* as a negative regulator of dehiscence. Observed expression patterns of *ALC* in pod are consistent with the previous findings that it has diffuse expression in valves of younger siliques (as reviewed in ref. 13). *SHP*s were shown to be specifically expressed in the VM starting before anthesis.[33]

Promoter-*GUS* analysis revealed that *ADPG1* and *ADPG2* are expressed predominantly in silique DZs just prior to or at dehiscence but are absent in valve.[8] The spot intensity of *ADPG1* was 6270 (±1051) and 21,985 (±2884), respectively, in DZ of *B. juncea* and *B. napus* at stage 2 and was at the background level in valve at the same stage in both *Brassica* cultivars. Thus, *ADPG1* was expressed 3.3-fold lower in stage 2 DZ (**Table S5**) of shatter resistant *B. juncea* than in shatter sensitive *B. napus* consistent with the direct involvement of *ADPG1* in dehiscence. Expression of *ADPG1* was also downregulated in silique of *shp1xshp2* relative to WT at all stages (**Table S11**).

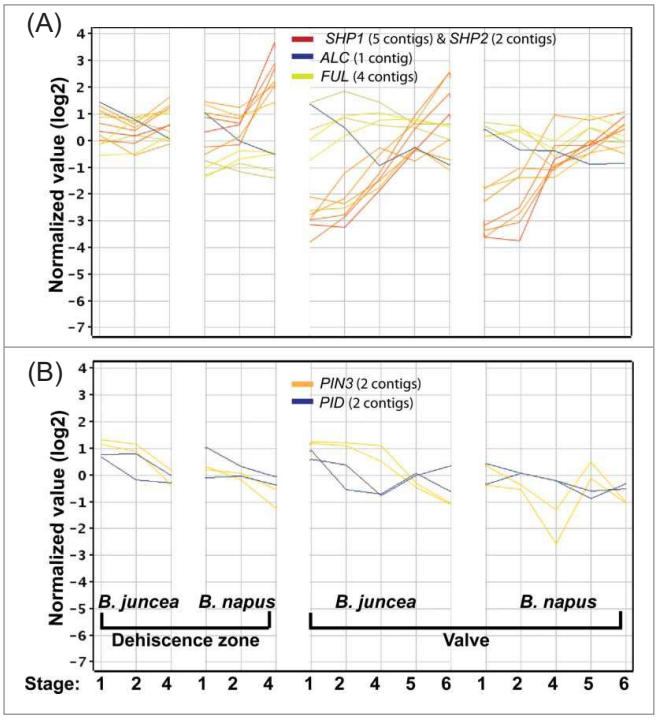

Figure 3. Transcript profiling of known dehiscence genes in DZ and valve of *B. juncea* and *B. napus* using *Brassica* microarrays. Expression of TFs *SHP1*, *SHP2*, *FUL* and *ALC* **(A)**. Expression of *PIN3* and *PID* **(B).**

Table 3. Differential expression of known dehiscence genes from 2 color *Arabidopsis* array data

		Arabidopsis: ful vs WT		
Gene name	**Locus ID**	**6 DPA**	**11 DPA**	**14 DPA**
IND (bHLH TF)	At4g00120	**12.93**	**12.77**	5.25
ADPG2 (endo-polygalacturonase)	At2g41850	1.43	4.17	**11.08***
ADPG1 (endo-polygalacturonase)	At3g57510	2.56	**4.95***	3.18*
FIL (YABBY1 TF)	At2g45190	2.43	4.27	1.21
SHP1 (MADS TF)	At3g58780	3.26	3.10	2. 18
PID (PINOID; protein kinase)	At2g34650	1.18	3.13	1.96
SHP2 (MADS TF)	At2g42830	1.94	2.72	2.71
FUL (bHLH TF)	At5g60910	0. 21	**0.16**	**0.13**
ALC (bHLH TF)	At5g67110	0.94	1.05	0.92
NST1 (NAM TF; ANAC043)	At2g46770	1.06	1.44	1.02
NST2 (NAM TF; ANAC066)	At3g61910	1.04		
NST3 (NAM TF; ANAC012)	At1g32770	1.22	0.79	0.59
PIN3 (auxin symporter)	At1g70940	0.65	1.77	1.08
JAG (zinc finger C2H2 type TF)	At1g68480	0.68	0.83	0.74
transducin family protein	At3g49400	1.29	1.13	0.96
QRT2 (polygalacturonase)	At3g07970		1.32	1.22
YAB3 (YABBY3 TF)	At4g00180	1.01	1.05	1.04
HEC3 (bHLH TF))	At5g09750	1.08	1.07	0.84

*Expression exceeded the detection limit of intensity value of 65,000. Fold changes ≥2 are shaded and ≥5 are in bold text.

The consistency of the differential expression of dehiscence genes in pods of *ful* vs. WT with previous studies encouraged us to examine in detail other differentially expressed genes. We identified cell wall related genes and TFs using functional annotation based on http://cellwall.genomics.purdue.edu/ for cell wall genes and PlnTFDB (plant transcription factor database) for TFs[34] (**Table S5**) that may be associated with the silique dehiscence. We selected these genes based on similarity to the expression patterns of *IND*, *ADPG1*, *ADPG2*, *SHP1* and *SHP2* in *ful* vs. WT and in DZ and valve *of B. juncea* vs. *B. napus* at stage 2.

Differences in silique lignin deposition and ultrastructure between *B. juncea* and *B. napus*

Previous studies on *B. napus* and *B. juncea* suggested that tensions generated between the non-lignified and rigid, lignified layers in the valve and VM precipitate silique dehiscence.[16] Upstream positive regulators of pod shatter *SHP1/2* promote lignification of a subset of VM cells.[4] Furthermore, in the *Arabidopsis alc* mutant, ectopically lignified cells in the inner VM create a "lignified bridge" between the lignified inner valve cell layers and the lignified replum vasculature, rendering *alc* siliques resistant to shatter.[15] We studied the progression of lignification and ultrastructural changes in silique development in both *Brassica* cultivars at stages 1, 2, and 4 and in dried mature siliques (**Fig. 4**). Circumferences (cross section) of siliques and sizes of most cell types of *B. juncea* were smaller than those of *B. napus* while the sizes of cells in en*b*, and septum (SE) were similar. There were 7-8 mesocarp (m) layer cells in both cultivars (**Fig. 4A-F**). At stage 1, M cells were rounded in shape in both

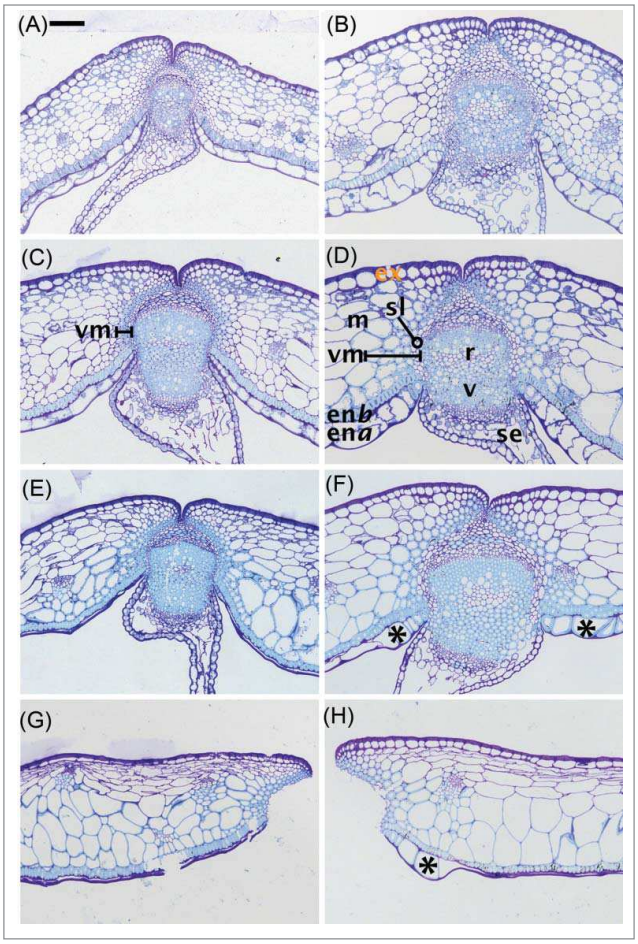

Figure 4. Degree of lignification and ultrastructural changes associated with the progression of *Brassica* silique dehiscence. Transverse sections were stained with toluidine blue O. Lignins stained blue and pectin and pectic substances stained purple. Sections of *B. juncea* silique at stage 1 (**A**), stage 2 (**C**), stage 4 (**E**) and mature-dried (**G**) and sections of *B. napus* silique at stage 1 (**B**), stage 2 (**D**), stage 4 (**F**) and mature-dried (**H**). Valves separated from replum of sections of mature-dried siliques during tissue preparation for microscopy. Abbreviations: en*a*, endocarp *a*; en*b*, endocarp *b*; ex, exocarp; m, mesocarp; r, replum; se, septum; sl, separation layer; v, vascular bundle; vm, valve margin. Scale bar, 100 μm. Stars depict remaining intact lignified cells after collapse of the en*a* layer at stage 4.

cultivars but became flattened and elongated at stage 2 in both the inner and the outer layers of M in *B. juncea* but only in outer layer of *B. napus*.

Toluidine blue staining revealed lignin in en*b*, M cells adjacent to SL and replum vasculature (v) in both cultivars as early as stage 1 (**Fig. 4A, 4B**). The degree of lignification in these cells, in addition to inner valve M cells, increased substantially at later stages of silique development. Nonetheless, the extent of lignification in these cells, specifically at stages 1 and 2 was lower in *B. juncea* than in *B. napus* (**Fig. 4A-D**) while conversely, lignin deposition was higher in stage 4 and mature-dry siliques of *B. juncea* than in *B. napus* (**Fig. 4E-H**). VM consists of lignified (LL) and non-lignified (SL) cells and there were 1-2 non-lignified cells in *B. juncea* and 3-5 in *B. napus* while the number of lignified cells was similar in both. Larger cell sizes and more cells in the VM of *B. napus* made the VM wider than that of *B. juncea*. The en*b* layer of *B. napus*, especially at stage 4, comprised 1-2 cell files whereas the en*b* of *B. juncea* consisted mostly of one cell file. Dissolution of the cells in the en*a* layer was observed at stage 4 leaving a few intact lignified cells close to both sides of the replum (indicated by asterisks in **Fig. 4**). In *B. juncea*, there were 1-4 very small surviving cells but there were 3-6 relatively large survivors in *B. napus* (**Fig. 4E-H**).

Careful examination of lignification at the inner VM cells in stage 4 revealed that the non-lignified cells extended a little beyond the en*a* toward the replum in *B. napus* while they ended, in most cases, just above the en*b* layer of *B. juncea* suggesting an *alc*-like lignified cell-bridge in *B. juncea* encompassing lignified en*b*, a few surviving-lignified cells of en*a* and lignified replum vasculature (**Fig. 4E, F**). This may be a significant factor in reducing shattering in *B. juncea*.

A previous study based on MRI revealed that during the early desiccation stage, shattering resistant *B. rapa* valves dried initially from the outside whereas *B. napus* valves dried initially from inside.[24] It was suggested that this drying pattern contributed to the different susceptibilities to shattering in the 2 cultivars. The increase in tension on the DZ is a product of senescence and desiccation, which together result in loss of flexibility and contraction of the valves. The microscopy results are consistent with preferential drying of *B. napus* siliques from the inside (**Fig. 4H**) since most of the en*a* layer had collapsed at the mature, dry stage but the exocarp (EX) layer remained hydrated, although there is some shrinkage of cells within the M layer. In *B. juncea*, early collapse of the en*a* layer is apparent at stage 4 (**Fig. 4E**), but by the mature, dry stage (**Fig. 4G**) the EX layer had collapsed and there was substantial shrinkage of M cells, suggesting rapid drying from the outside. Therefore, the most obvious difference in silique drying between the 2 species is the relative resistance of the outer EX and M cells to water loss in *B. napus*. This asymmetric drying in *B. napus* may contribute toward additional tension on the DZ as described previously.[24]

Shikimate, phenylpropanoid and monolignol biosynthesis pathways are strongly downregulated in *B. juncea* relative to *B. napus*

The shikimate pathway links primary and secondary metabolism and products arising from the pathway include lignins (reviewed in ref. 35). As noted above, lignification plays an important role in silique dehiscence[4,16] and we have described significant differences in silique lignin deposition between *B. juncea* and *B. napus* (**Fig. 4**). Moreover, lignification occurs in the whole inner valve of the *ful* mutant since the valves manifest replum-like characteristics, and as a result siliques fail to dehisce .[17] Therefore, we compared genes of these pathways in *Arabidopsis ful* vs. WT and from DZ and valve of *B. juncea* vs. *B. napus*.

The shikimate pathway consists of 7 enzymes, and 9 genes coding for pathway enzymes were substantially downregulated in *B. juncea* compared to *B. napus* (**Table S6**). The final product of the shikimate pathway is chorismate, which is converted into

Table 4. Differential expression of genes encoding enzymes of phenylpropanoid pathway and biosynthesis of monolignol and sinapate ester (functional annotation based on http://cellwall.genomics.purdue.edu/) from 2-color *Arabidopsis* microarray data

					Stages: B. juncea vs. B. napus					
		Arabidopsis: ful vs. WT			DZ*	valve*	valve**			
Gene name	**Locus ID**	**6 DPA**	**11 DPA**	**14 DPA**	**2**	**2**	**3**	**5**	**6**	**Pathway**
PAL1; phenylalanine ammonia-lyase 1	At2g37040	0.99	0.90	0.33	0.97	1.13	0.72	0.22	**0.16**	Phenylpropanoid
PAL2; phenylalanine ammonia-lyase 2	At3g53260	1.46	1.26	0.49			0.31	0.24	0.45	Phenylpropanoid
PAL4; phenylalanine ammonia-lyase 4	At3g10340	0.80	1.20	1.86	0.57		**0.13**	**0.03**	**0.05**	Phenylpropanoid
C4H; Trans-cinnamate 4-hydroxylase; CYP73A5	At2g30490	1.36	1.18	0.86	0.44	0.41	0.46	0.85	1.90	Phenylpropanoid
4CL1; 4-coumarate coenzyme A ligase 1	At1g51680	0.83	1.22	1.01	0.32	0.39	0. 16	**0.08**	**0.08**	Phenylpropanoid
4CL3; 4-coumarate coenzyme A ligase 3	At1g65060	1.03	0.80	0.34	1.48	1.21	1.32		0.24	Phenylpropanoid
4CL4; 4-coumarate coenzyme A ligase 4	At3g21230	0.95	0.90	1.14	0.57	0.56	0.48	0. 18	0.29	Phenylpropanoid
4CL-like1	At1g20510	1.08	0.41	0.64	1.87	1.35	1.28	0.77	0.37	Phenylpropanoid
HCT; Hydroxycinnamoyl-CoA: shikimate/quinate hydroxycinnamoyltransferase	At5g48930	1.64	1.56	1.25	1.55	1.58	0.74	0.36	0.37	Phenylpropanoid
C3H1; p-coumarate-3-hydroxylase; CYP98A3	At2g40890	1.04	1.07	0.92	0.51	0.53	0.32	0.27	0.58	Phenylpropanoid
CCoAOMT1; caffeoyl-CoA 3-O-methyltransferase 1	At4g34050	0.98	1.32	1.77	0.42	0.45	0.76	0. 21	0.55	Phenylpropanoid
CCR-like5; cinnamoyl-CoA reductase-like5	At5g58490	0.94	0.76	0.79	1.55	1.58	2.02	0.82	0.26	Monolignol
F5H1; ferulate-5-hydroxylase 1; CYP84A1	At4g36220	0. 23	0.58	0.37	0.44	0.50	0.35	0.88	3.19	Monolignol
COMT; caffeic acid O-methyltransferase	At5g54160	0.67	1.16	1.13	0.34	0.40	0.41	0.16	0.21	Monolignol
CAD4; cinnamyl alcohol dehydrogenase 4	At4g37980	1.81	0.49	0.58	0.58	0.55		**0.06**	**0.14**	Monolignol
CAD6; cinnamyl alcohol dehydrogenase 6	At4g34230	0.97	1.39	0.99	0.53	0.63	0.73	0.40	0.34	Monolignol
CCoAOMT6;; caffeoyl-CoA 3-O-methyltransferase 6	At1g67980	1.19	0.91	1.66	0.94	1.13	2.00	3.41	2.96	Phenylpropanoid
O-methyltransferase Family 2 Protein	At4g35150	0.80	0.63	0.63	1.26	1.02		1.73	3.20	
O-methyltransferase Family 2 Protein	At4g35160	0.88	0.93	0.99	1.34	0.99		1.12	3.50	
CAD5; cinnamyl alcohol dehydrogenase 5	At4g37990	**9.62**	3.61	1.24	1.09	0.74	1.32	6.06	4.99	Monolignol
COMT-like1	At1g21100				1.08	0.96	3.33	8.58	**33.72**	Monolignol
COMT-like2	At1g21110	0.68	0.51	0.43	1.11	0.96	2.76	**9.94**	**22.64**	Monolignol
COMT-like3	At1g21120	0.59	0.54	0.67	1.09	1.00		5.52	5.28	Monolignol
COMT-like4	At1g21130	0.62	0.67	0.66	1.15	0.86	5.73	**10.29**	**29.57**	Monolignol
sinapoylglucose:malate sinapoyltransferase (SNG1)	At2g22990	1.15	1.24	0.63	2.94	3.32	4.89	5.21	1.34	Sinapate ester
peroxidase	At3g17070	0.38	0.43	0. 24	0.76	1.23	0.73	0.49	0.32	
PER3 = Rcl3	At1g05260	1.40		0.81	0. 20	0. 24		0.45	0.52	
peroxidase	At3g28200	1.28	0.87	0.68	2.00	2.10	2.14	1.34	2.79	
PER17	At2g22420	2.08	1.46	0.60	2.14	2.05	1.92	2.97	3.33	
peroxidase	At5g14130	1.26	2.05	1.39	1.09	0.98	2.97	2.22	3.43	
PER21	At2g37130	1.28	0.35	0.58	3.10	9. 17	1.94	1.65	4.22	
peroxidase	At5g64120	3.83	0.82	0.70				**26.17**	**14.11**	
PER12	At1g71695	0.37	1.92	1.65	2.17	1.73	1.88	**9.71**	**27.56**	
peroxidase	At4g08770	0.85	0.79	0.97	2.26	1.69	5. 04	**19.19**	**57.37**	
PERx34	At3g49120	0.32	0.29	0.81	1.42	0.95	2.98	**14.12**	**67.53**	
LAC15; Laccase	At5g48100	0.61	2.11	2.12	0.81	0.81		5.94	**10.63**	
LAC1; Laccase	At1g18140	0.94	0.90	0.93	0.93	0.96	0.33	0.25	0.44	

*DZ and valve dissected under microscope. **Manually dissected valve and septum. Fold change $\geq$5 are shaded and $\geq$10 have bold text.

Table 5. Significant pathways derived by Wilcoxon rank sum Test (p-value cut-off: ≤0.05) in MapMan[44] from *Arabidopsis* microarray data

		B. juncea* vs. *B. napus			***ful* vs. WT**						***shp1* x *shp2* vs. WT**			***alc* vs. WT**			**Genotype**
		valve			**pod**			**whole silique**			**whole silique**			**whole silique**			**Tissue type**
Bin#	**Assignment (MapMan)**	**3**	**5**	**6**	**6 DPA**	**11 DPA**	**14 DPA**	**3**	**5**	**6**	**3**	**5**	**6**	**3**	**5**	**6**	**Development stage**
35	Not assigned		646	933			2				43						
27	RNA	8	19	56	117	139								6	6		
26	Miscellaneous	28	89	167	3	28	15		9	5				6			
34	Transport	14	26	33			15		8					14	4		
20	Stress		21	6			26		45						18		
16	Secondary metabolism	3	49	54		4	13							3			
33	Development		5	11	11	7			6					2		3	
1	Photosynthesis	3	19	43	2	6	2										
29	Protein		15	35	25	5						32	9		2		
11	Lipid metabolism	6	19	32	4	8			5								
10	Cell wall	2	3	11		10	7						4				
17	Auxin	20			31	12						2					
31	Cell				2												
21	Redox	13	14	11										3			
2	Major CHO metabolism	5		24		9											
30	Signaling	4	20	8													
17	Ethylene	2	13	14													
13	Amino acid metabolism			10					2								
15	Metal handling			14													
17	GA																
12	N-metabolism			3	4	2											
18	Co-factor and v itamine metabolism			7													
25	C1-metabolism		2	2													
3	Minor CHO metabolism			3													
14	S-assimilation			3													
17	CK			3													
9	Electron transport																
17	ABA					2											
23	Nucleotide metabolism																

multiple products, including lignin. Transcript downregulation was observed in *B. juncea* compared *to B .napus* for 5 genes involved in chorismate metabolism.

Next, we compared the expression of genes involved in monolignol biosynthesis in the *Brassica* cultivars. Expression of 27 genes involved in the pathway were detectable by microarray analysis and 16 of these were moderately to highly downregulated in valve and DZ of *B. juncea* compared to *B. napus* (**Table** 4). It was clear that monolignol (mainly coniferyl alcohol/G unit and coumaryl alcohol/H unit) biosynthetic genes were downregulated in *B. juncea* relative to *B. napus*. However, transcripts of sinapoyl glucose: malate sinapoyl transferase (*SNG1*) stayed upregulated up to stage 5 and transcripts of CCoAOMT6, O-methyltransferase Family 2 Protein, CAD5, and COMT-like1/2/3/4 were highly upregulated, especially in stages 5 and 6 in *B. juncea* relative to *B. napus* indicating enrichment of sinapoyl alcohol (S) units in lignin polymers and/or the formation of sinapoyl malate ester.[36] Interestingly, only a few monolignol biosynthetic genes were differentially expressed in *ful* vs. WT comparisons (**Table** 4). However 10 of the 16 upregulated genes in the *Brassica*s were also downregulated in *alc* and *shp1xshp2* relative to WT (**Table S11**).

After synthesis, monolignols are transported from cytoplasm to the cell wall and lignin is formed through polymerization of the monolignols involving peroxidases, laccases, polyphenol oxidases, and coniferyl alcohol oxidase.[37] Peroxidases and laccases belong to large families in *Arabidopsis* and hence we only examined cell wall related peroxidases and laccases. Transcripts of 10 cell wall related peroxidases and one laccase were highly upregulated – especially in stages 5 and 6 in *B. juncea* relative to *B. napus* and this is correlated with our microscopy data (**Fig. 4E-H**) suggesting increased lignifications in stage 4 and dry-mature silique in *B. juncea* relative to *B. napus*.

Remodeling of cell wall components during silique dehiscence

Plant cell walls are composed of cellulose microfibrils coated by xyloglucans and embedded in a matrix of pectic polysaccharides.[38] Pectins constitute a complex family of galacturonic acid

(GalA)-rich (70% of pectin) polysaccharides. They are abundant in the primary cell wall and in the intercellular matrices of middle lamellae in which they form a gelling matrix for cell-cell adhesion. Homogalacturonans (HGs) are the most abundant pectins (65%) and are synthesized in the Golgi apparatus mostly as methylester precursors (60%). Methylated HGs are secreted into the apoplast, where they are deesterified by pectin methylesterase (PME) to form negatively charged pectate. Pectates are cross-linked with each other through calcium ions to form a gel.

Pectin modification enzymes

PMEs generate deesterified HGs, which are degraded preferentially by endo-PGs.[39] Therefore, PMEs and PGs are thought to act together in the degradation of pectins and are involved in cell wall breakdown during silique dehiscence.[8,40,41] While screening for cell-wall genes whose expression was reminiscent of *ADPG1* and *ADPG2* we identified homologs of 4 *PME*s (At1g11580, At2g36710, At5g26810 & At3g59010) that were highly upregulated in *ful* relative to WT and were downregulated in DZ and valve of *B. juncea* relative to *B. napus* (**Table S5**). Conversely, 2 *PME*s (At3g62170 & At1g53840) showed the opposite expression profiles in both *ful* vs. WT and *Brassica* cultivar comparisons. PME can be inactivated by PME inhibitors (PMEIs) and expression of *PMEI1* (At1g48020) was downregulated in *ful* relative to WT, but was undetectable in *Brassica*. Overall, PMEs seemed to be associated with shattering.

Besides endo-PG *ADPG1*, 4 other *PG*s (At1g80170, At1g19170, At3g16850 and At5g41870) were highly downregulated in *B. juncea* relative to *B. napus* but unlike *ADPG1*, these genes were not upregulated in pods of *ful* vs. WT and therefore may not be directly involved in dehiscence or may not be regulated by *IND*. Transcript of PG - inhibiting protein (*PGIP1*) that inhibits fungal PGs,[42] was highly upregulated in DZ and valve of *B. juncea* relative to *B. napus*.

Pectate can be degraded by pectate lyase (PL). Eight *PL*s were differentially regulated and 5 (At1g14420, At3g01270, At3g09540, At3g55250 & At5g15110) were downregulated and 3 (At1g04680, At4g24780 & At5g63180) were upregulated in both *ful* vs. WT and *Brassica* cultivar comparisons. Pectin acetylesterases (PAEs) deacetylate homogalacturonan polymers and thus solubilize pectin facilitating the access of PL to substrate. Two PAE genes were up- and 3 genes were downregulated in *B. juncea* compared to *B. napus*.

The enzyme β-galactosidase (BGAL) degrades structural pectins, xyloglucans or arabinogalactoproteins in plant cell walls and 3 *BGAL*s (*BGAL1/3/6*) were upregulated by 2-6 fold in *B. juncea* relative to *B. napus*.

There is a unifying pattern in most of the pectin-related genes that can be related to pectin degradation and consequently to shattering – especially in the *Brassica* data. There is a tendency for reduced expression of *PG*s, *PME*s and *PL*s associated with pectin breakdown in *B. juncea* vs *B. napus* comparisons (and for PGIP1 to increase). This could suggest stronger middle lamellae, contributing to reduced shattering. Alternatively, reduced pectin degradation might be a consequence of fewer SL cells in *B. juncea* than in *B. napus* (**Fig. 4**).

Xyloglucan endotransglucosylase/hydrolases (XTH)

XTHs have dual activities as endotransglucosylase (XET) and endohydrolase (XEH) and can strengthen or loosen cell walls under different circumstances. They belong to a large family of 33 genes[43] and 7 *XTH*s (*XTH3/6/7/8/10/16/29*) were differentially expressed (**Table S5**). In our microarray analysis, expression levels of all 7 were very low in *Brassica,* and in *Arabidopsis*, expression of all except *XTH3/6/10* were very low. In *Arabidopsis*, expression of *XTH3* increased only in *ful* pod at 11 DPA and 14 DPA; *XTH6* increased in WT pods at 6 DPA and of *XTH10* increased only at 14 DPA in WT. In addition to low expression level, differential expression of XTHs exhibited noclear pattern in relation to pod dehiscence.

Enriched metabolic pathways

Expression data was mapped on to biological pathways using MapMan.[44] We documented some key processes in silique development (**Tables 6**, **7**). Genes in individual biochemical pathways were initially annotated according to the Plant Metabolic Pathway Database (http://www.plantcyc.org/), Cell Wall Genomics (http://cellwall.genomics.purdue.edu/) and MapMan and then updated from the published literature.

Photosynthesis

Both seed and silique lose chlorophyll and photosynthetic activity during development. Transcripts of 65 photosynthetic genes were downregulated in pod of *ful* compared to WT indicating that WT leaf-like valves became non-photosynthetic and VM-like in *ful* (**Fig. 5**). These genes were also downregulated in *B. juncea* vs. *B. napus* comparisons and in whole siliques of *alc* compared to WT but were not differentially regulated in whole siliques of the *shp1xshp2* vs. WT comparison suggesting that changes in photosynthetic genes are not directly related to dehiscence.

Senescence

Silique dehiscence shows similarities in gene expression and hormone signaling with senescence, wounding and defense.[16,31] Genes such as *SAG12*, *AUTOPHAGY 8* (*APG8*), *APG12*, *PDF1.2*, *VSP2*, and *LOX2* that are correlated with cell death and organ senescence were upregulated in yellowing silique wall of *Arabidopsis*.[31,45] Interestingly, genes of 6 plant defensin fusion proteins (PDF), PDF1.1/1.2a/1.2b/1.2c/1.3/2.3, were highly expressed in DZ and valve of *B. napus* and these *PDF*s along with *PDF1.5* were downregulated strongly in *B. juncea* (**Table 7**). *PDF1.1/1.2b/1.2c* were also downregulated in *alc* but were upregulated in *ful* relative to WT (**Table S1**). Five autophagy genes *APG6*, *APG8c*, *APG8f*, *APG12a* and *APG12b* were also highly downregulated in *B. juncea* relative to *B. napus* in all tissues at all stages. Senescence marker genes *SAG12* and *SAG21* were downregulated in *B. juncea* relative to *B. napus* at early and later stages of silique development, respectively. Both *SAG12/21* were highly

Table 6. Significant pathways derived by Wilcoxon rank sum test (*p*-value cut-off: ≤ 0.05) in MapMan[44] from *Brassica* (Combimatrix) microarray data

		B. juncea			***B. napus***			***B. juncea***					***B. napus***					**Genotype**
		Dehiscence zone						**Valve**										**Tissue type**
Bin#	Assignment (MapMan)	1	2	4	1	2	4	1	2	4	5	6	1	2	4	5	6	Development stage
35	Not assigned	235						269			268					159	544	
29	Protein	180			2	2	22	208	96	115	83		8	3		17	133	
34	Transport	4		4	50			4	11	5	61	114	55	3		88	159	
20	Stress	90	74		77	8		84	66	12	3	12	92	8	26		119	
26	Miscellaneous	36	20	6	38	6	15	34	18	17	44	40	45	8	10	40	37	
10	Cell wall	69	14		74		9	64	11			10	53	9	9	6	2	
33	Development	28		8			22	39	8	6	4	18	19		31	21	45	
11	Lipid metabolism	12	8	12	7		10	9	12	5		7	9		10	8	13	
27	RNA	5		45	5		3	15		3	6	16	3			2	11	
1	Photosynthesis	8	2	3			22	19	2	2		24	7					
13	Amino acid metabolism				17					19	2	3				3	65	
31	Cell								7			13			14	37	37	
17	Hormone metabolism: auxin	2					4	2		4	11	10				11	16	
18	Hormone metabolism: ethylene			4				3		4	5	6				5	6	
16	Secondary metabolism			6			2	2	6		6	2			3	15		
30	Signaling	4	3					4			2					13	2	
24	Biodegradation of Xenobiotics											5				6	5	
21	Redox	3		4				6			6							
6	Gluconeogenesis/glyoxylate cycle										2	6				6	5	
18	Hormone metabolism: salicylic acid			3					2		3	3					3	
28	DNA						4					3						
2	Major CHO metabolism						2				3					3		
18	Hormone metabolism: gibberelin	4						3										
3	Minor CHO metabolism											2					4	
9	mit. electron transport/ATP synthesis					2												
18	Hormone metabolism: jasmonate														2			
4	Glycolysis																3	
23	Nucleotide metabolism																	
8	TCA						2											
12	N-metabolism																	
17	Hormone metabolism: cytokinin										2							

downregulated in *ful* vs. WT but were upregulated in *shp1 X shp2* vs. WT and *alc* vs. WT comparisons (**Table S1**) suggesting *SAG12/21* are either unlinked to pod shattering and/or not regulated by *SHP*s and *ALC*. However, marker genes *VSP1/2* of ethylene and jasmonate signaling pathways were downregulated in *alc* vs. WT and *shp1xshp2* vs. WT comparisons (**Table S1**). Therefore, downregulation of *PDF*s, *APG*s, and *SAG*s suggests that delayed and/or reduced senescence may contribute toward reduced dehiscence in *B. juncea*.

Phytohormones

Auxin: Significant pathway analysis in MapMan revealed differentially regulated genes associated with auxin and ethylene (**Tables 5**, **6**). Recent results have documented a local auxin minimum required for the specification of the VM SL.[14] Therefore, we examined the expression of genes involved in auxin biosynthesis, transport and signaling. Several genes coding for auxin biosynthetic enzymes were strongly downregulated in *B. juncea* relative to *B. napus* (**Table S7**). IAA biosynthetic genes such as *NIT1/2/3*, *IBR3*, *ILL6* and *ILR1* were also downregulated in *shp1xshp2*, *alc* and *ful* in comparison to WT (**Table S1**). The majority of IAA in *Arabidopsis* is found conjugated as glycosyl esters or amide-linked IAA-conjugates, some of which could release free IAA upon hydrolysis.[46,47] IAA-conjugates play an important role in IAA metabolism and homeostasis and in *Arabidopsis*, 90% of the conjugated IAAs are amide-linked and are formed by indole-3-acetic acid amido synthetases, which belong to the *GH3* gene family of auxin primary response genes. Genes catalyzing the formation of IAA conjugates including several *GH3*s and *UDP-GLUCOSE TRANSFERASE* (UGT1/At1g05560) were highly upregulated in *B. juncea* relative to *B. napus* indicating the synthesis of storage forms of IAA (**Table S7**).[46,48] In contrast, most of these auxin conjugating genes were downregulated in *ful* vs. WT.

A proper auxin response is dependent on the delivery of IAA to target cells by polar transport involving influx and efflux carriers. The efflux carriers *PIN3/4* as well as the influx carrier *AUX1* and transporter *PGP19* were downregulated whereas 2 auxin efflux carrier family proteins (At1g76520, At2g17500) were upregulated in *B. juncea* compared to *B. napus* (**Table S7**). The expression patterns of these transporter genes were reversed in *ful* vs. WT compared to *B. juncea* vs. *B. napus*, suggesting that their expression is linked to dehiscence.

Table 7. Transcript profiles of senescence related genes of *Arabidopsis* and *Brassica* cultivars in various tissues during silique development

		DZ*: B. juncea versus B.			Valve*: B. juncea vs. B. napus					
Gene name	**Locus ID**	**1**	**2**	**4**	**1**	**2**	**4**	****5**	****6**	**: Stages**
APG6	AT3g61710	↓8.49	↓7.87	↓8.04	↓10.56	↓9.66	↓16.2	↓18.68	↓48.93	
APG8c	AT1g62040	↓3.95	↓5.22	↓12	↓5.54	↓21.78	↓5.84	↓6.03	↓14.73	
APG8f	AT4g16520	↓10.71	↓16.66	↓9.01	↓20.12	↓57.44	↓19.28	↓60.2	↓115.04	
APG12a	AT1g54210	↓2.36	↓3.97	↓2.82	↓2.55	↓3.53	↓7.57	↓6.52	↓42.78	
APG12b	AT3g13970	↓6.9	↓7.49	↓5.71	↓17.37	↓11.07	↓12.35	↓43.51	↓24.88	
PDF1.2a	AT5g44420	↓107.1	↓311.7	↓33.39	↓355	↓306.8	↓129.4	↓648.7	↓683.2	
SAG12	AT5g45890				↓1.94	↓8.63				
SAG21	AT4g02380		↑4.09	↓2.03			↓6.12		↓2.36	
					B. Juncea vs. B. napus					
Arabidopsis array data:		**Arabidopsis: ful vs. WT**			**DZ***	**valve***	**valve****			**: Stages**
Gene name	**Locus ID**	**6 DPA**	**11 DPA**	**14 DPA**	**2**	**2**	**3**	**5**	**6**	
APG8c	**At1g62040**						↓17.29	↓23.42	↓11.55	
PDF1.1	At1g75830			↑9.62	↓2.31	↓2.22	↓1.68	↓5.68	↓4.29	
PDF1.2a	AT5g44420				↓4.88	↓5.13	↓3.73	↓21.71	↓24.93	
PDF1.2b	At2g26020			↑1.9	↓4.79	↓3.73		↓4.94	↓3.85	
PDF1.2c	At5g44430			↑2.75	↓3.15	↓3.31		↓5.57	↓3.3	
PDF1.3	At2g26010				↓2.88	↓2.68		↓3.85	↓2.96	
PDF1.4	At1g19610				↓3.41	↓2.27		↑5.2	↑8.58	
PDF1.5	At1g55010		↑2.39	↑1.96			↑1.8	↓14.49	↓18.57	
PDF2.3	At2g02130				↓3.64		↓4.41	5.29		

↑ : fold upregulated. ↓ : fold downregulated. In Combimatrix data, fold changes of multiple contigs for the same gene are averaged. *DZ and valve dissected under microscope. **Manually dissected valve.

Auxin responses involve ubiquitination and subsequent degradation of Aux/IAA transcriptional repressor proteins resulting in the release of auxin response factor (ARF) proteins which either activate or repress auxin-regulated genes.[47] In the absence of auxin, ARFs are sequestered and inactivated by Aux/IAAs. There are 22 ARFs and 29 AUX/IAAs in *Arabidopsis*. No clear pattern of expression was apparent for ARFs (**Table S7**). Expression of *IAA*s including *IAA9/10/12/13/17/18/26* were down regulated and *IAA8/31* were up regulated in *B. juncea* relative to *B. napus* (**Table S7**). This suggests that, similar to auxin biosynthesis and transport, auxin signaling was predominantly repressed in *B. juncea* compared to *B. napus*.

Ethylene: Ethylene has a role in many processes including organ abscission, senescence and stress.[49] Ethylene is synthesized from methionine (Met) by 3 enzymes: S-adenosyl-L-Met (AdoMet) synthetase, 1-amino-cyclopropane-1-carboxylate (ACC) synthase (ACS) and ACC oxidase (ACO). ACS catalyzes the first committed step and, in most instances, is rate limiting. Several ethylene biosynthetic genes were highly upregulated in all tissues and stages tested in *B. juncea* compared to *B. napus* including *SAM1*, 5 *ACS*s, *ACO1, ACO2* and 4 others *ACO*s (**Table S11**). Ethylene biosynthesis is regulated, in part, by *ETO1* and 2 *ETO1*-like genes *EOL1* and *EOL2* negatively regulate ACS activity and hence ethylene production.[50] *EOL1* was downregulated in *B. juncea* relative to *B. napus* (**Table S8**). Upregulation of several biosynthetic genes and downregulation of *EOL* indicates that ethylene biosynthesis is upregulated in shatter resistant *B. juncea* relative to shatter sensitive *B. napus* which is consistent with previous results that *B. juncea* siliques produced considerably higher ethylene inside siliques than *B. napus* throughout silique development.[27]

In the absence of ethylene, its receptors activate the Raf-like protein kinase CTR1 (MAPKKK), which is a negative regulator of ethylene action. Two among its 5 receptors, *ETR1* and *ETR2,* were downregulated and *CTR1* was upregulated in *B. juncea* compared to *B. napus* (**Table S8**). Among the downstream effectors, *EIN2* and *EIN3* are positive regulators of ethylene action and were downregulated in *B. juncea* more than in *B. napus*. *EIN2* is upregulated in *ful* vs. WT. Taken together, the downregulation of 2 receptors *ETR1* and *ETR2* and 2 positive regulators *EIN2* and *EIN3* and upregulation of negative regulator *CTR1* indicate that, in contrast to biosynthetic genes, ethylene signaling was downregulated in *B. juncea* more than in *B. napus*. Ethylene regulates its own biosynthesis through a positive feedback control.[51] Therefore, down regulation of ethylene signaling may act as a positive feedback for the induction of ethylene biosynthesis. In *Arabidopsis*, *ACO2* and a putative *ACO* were downregulated in *shp1xshp2* and *alc* relative to WT suggesting reduced ethylene production in non-shattering genotypes (**Table S11**).

Jasmonic acid (JA): The bioactive form of JA (e.g., jasmonoyL-isoleucine, JA-Ile) plays an important role in wounding and pathogen invasion (for reviews, see refs. 52, 53). In our microarray data, downregulation of marker genes for JA signaling such as *PDF1.2a/b/c* in *B. juncea* relative to *B. napus* (**Table 7**) prompted us to look closely JA biosynthesis and signaling. JA is derived from α-linolenic acid (18:3) which can be generated by at least 3 enzymes FAD3, FAD7 and FAD8. *FAD3* and several other genes

Figure 5. Heat map representation of expression of photosynthetic genes derived from *Arabidopsis* microarrays.

coding for JA biosynthetic enzymes, including 4 lipoxygenases (LOX1/2/4), 3 allene oxide cyclases (AOC1/2/3), and 12-oxophytodienoate reductase (DDE1) were upregulated in *B. juncea* relative to *B. napus* (**Table S9**). In contrast to JA biosynthesis, genes *JAR1* and *JMT* for the formation of JA-Ile and methyl jasmonate (MeJA), respectively, were downregulated in *B. juncea* relative to *B. napus*. Like auxin signaling, JA-Ile action results in the ubiquitination and subsequent degradation of JAZ repressors, which releases JA signaling. Positive regulators *COI1* and *MYC2* expressions were downregulated whereas negative regulators *JAZ1/2/8/9/10* were upregulated in *B. juncea* relative to *B. napus* implying a suppression of JA signaling in *B. juncea*. This is consistent with the suppression of JA marker genes: *PDF*s and *VSP2* in *B. juncea*, *alc* and *shp1 x shp2* (**Table 7**; **Table S11**). Therefore, similar to ethylene, down regulation of JA signaling may in turn activate JA biosynthetic genes through positive feedback. JA biosynthetic genes *FAD3*, *LOX1* and *LOX2* were downregulated in *shp1 x shp2* vs. WT (**Table S9**).

ABA: ABA is a key phytohormone in water stress responses. Several genes of ABA biosynthesis including *NCED*, *AAO3* and *ABA3* were induced and 2 genes coding for the catabolic enzyme ABA 8′-hydroxylase were repressed in *B. juncea* relative to *B. napus* and in *ful* vs. WT (**Table S10**).[54] Induction of ABA biosynthesis correlates with the high expression of SSP, oleosin and LEAs and down regulation of photosynthetic genes in pods of *B. juncea* and *ful* as described above and similar effects of ABA have been described previously.[55-57] ABA induces the expression of many genes that are important for adaptation to abiotic stresses.[57] The expression of these stress related genes and of TFs involved in mediating ABA responses such as *ABF2/3/4* are upregulated in *B. juncea* relative to *B. napus* and in *alc*, *shp1xshp2* and *ful* relative to WT (**Tables S10, S11**) indicating stronger adaptive responses to desiccation in shatter-resistant genotypes.

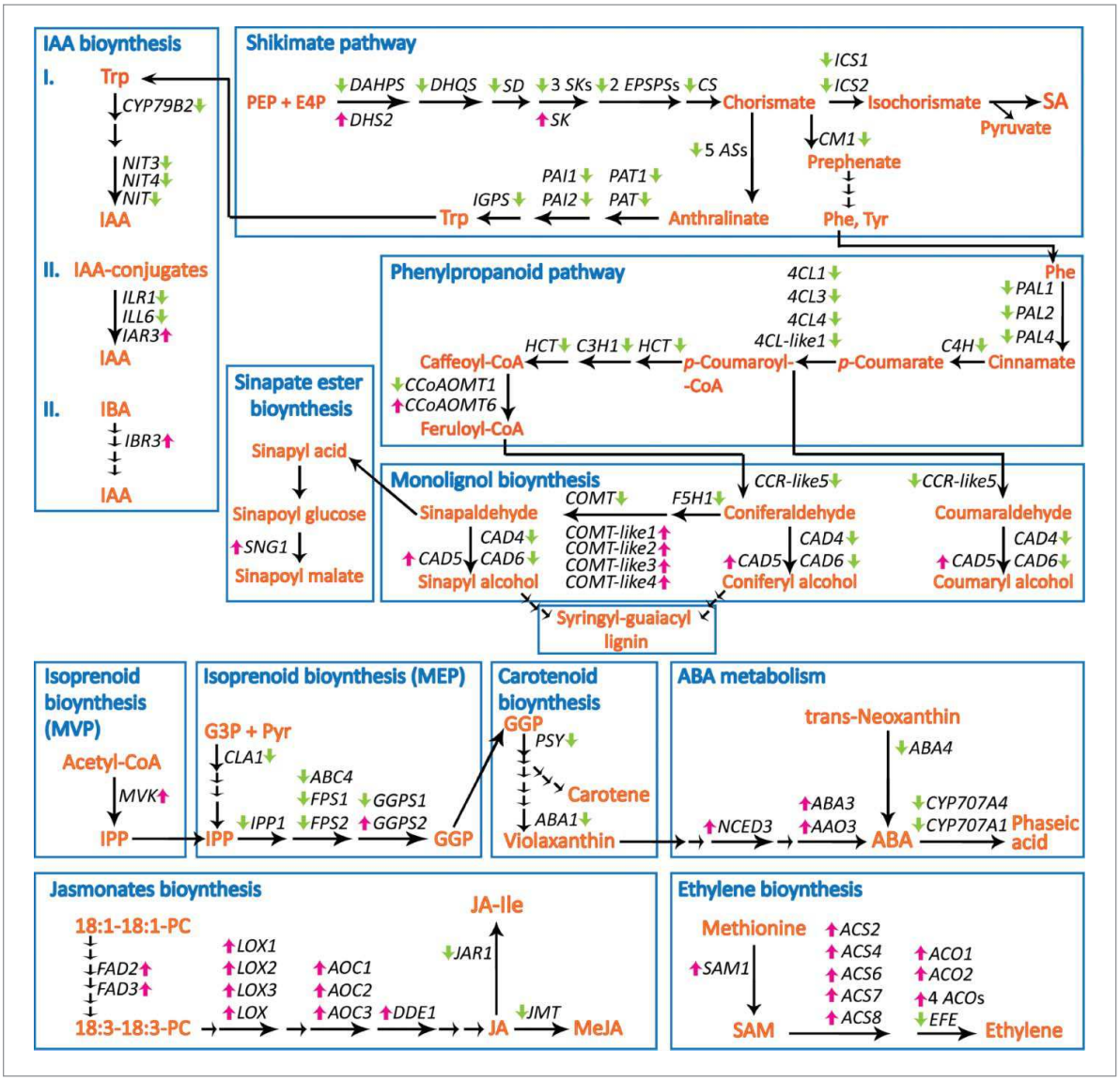

Figure 6. Illustration of the metabolic pathways and genes that were differentially affected in siliques between *B. juncea* and *B. napus*. Unabbreviated gene names and AGI numbers are listed in respective pathway-**Table 4** and **Tables S6** to **S11**. Other abbreviations for each pathway are as follows. IAA biosynthesis: IAA, indole-3-acetic acid; IBA, indole-3-butyric acid. Shikimate pathway: PEP, phospho-enol-pyruvate; E4P, erythrose 4-phosphate. Isoprenoid biosynthesis: MVP, mevalonate pathway; IPP, isopentenyl diphosphate; MEP, methyl erythritol phosphate pathway; G3P, D-glyceraldehyde-3-phosphate; Pyr, pyruvate; GGP, geranylgeranyl diphosphate. Carotenoid biosynthesis: GGP, geranylgeranyl diphosphate. Jasmonates biosynthesis: 18:1-18:1-PC, 1,2-dioleoylphosphatidylcholine; 18:3-18:3-PC, 1,2-dilinolenoylphosphatidylcholine; JA, jasmonic acid; MeJA, methyl jasmonate; JA-Ile, JA-isoleucine. Ethylene biosynthesis: SAM, S-adenosyl methionine.

Discussion

Expression of upstream regulators such as *SHP1/2* and *IND* were upregulated in *ful* vs. WT comparisons (**Table 3**) whereas *FUL* and *ALC* were upregulated and *SHP1/2* downregulated in DZ of *B. juncea* vs. *B. napus* comparison (**Fig. 3A**) (*IND* was absent from the Brassica array). *SHP1/2* and *FUL* regulate silique dehiscence and their expression is consistent with the observed differences in shattering between the 2 species. In general, our microarray data showed that expression of dehiscence-related genes in *ful* vs. WT were opposite to that in *B. juncea* vs. *B. napus*. However, there were some exceptions to this relationship. Similarities between some differentially expressed genes in the *B. juncea* vs. *B. napus* and *ful* vs. WT comparisons might reflect the fact that *ful* siliques are also relatively resistant to dehiscence due to loss of VM identity and ectopic lignin deposition in the entire inner valve.

Among the known downstream shattering genes, *ADPG1/2* were upregulated and *NST3* was downregulated in *ful* relative to WT, whereas both *ADPG1* and *NST1/3* were downregulated in *B. juncea* vs. *B. napus* and *shp1xshp2* vs. WT. Expression of these genes appears to be reduced in most shattering-resistant

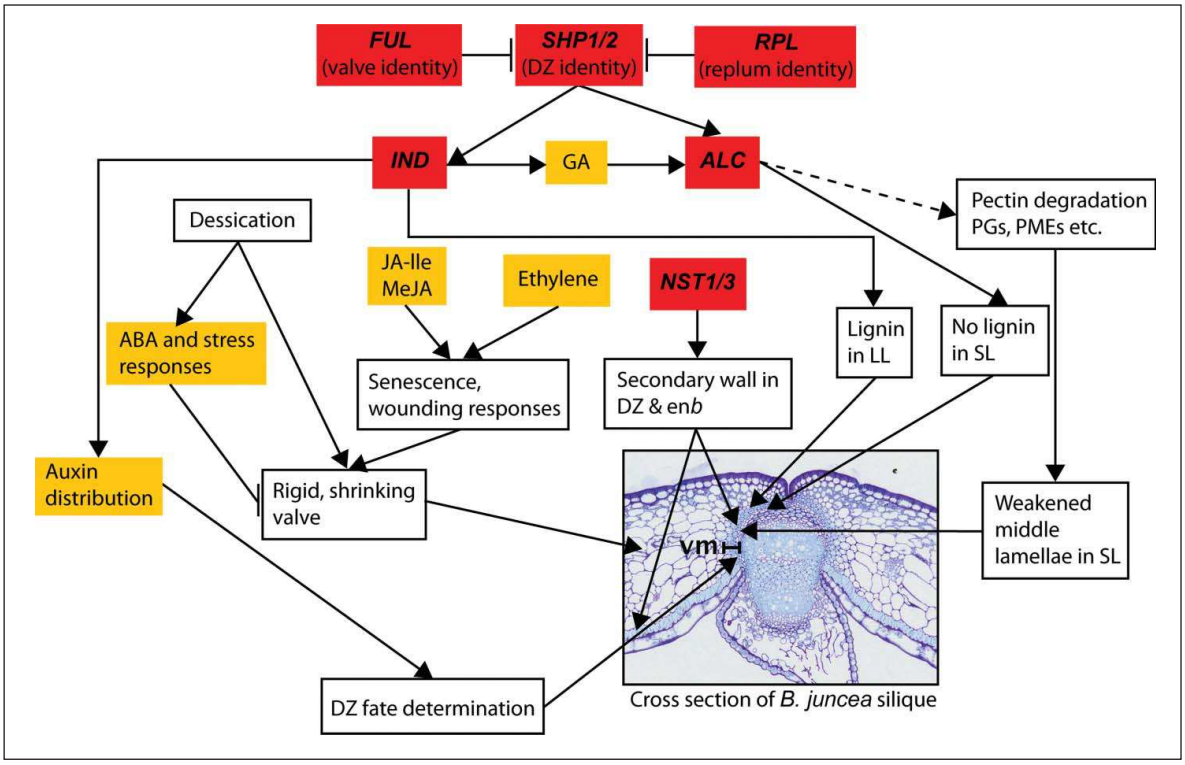

Figure 7. Model summarizing the biological processes, hormones and regulatory proteins controlling silique dehiscence in Brassicas. A cross-section of a *B. juncea* silique from **Fig. 4c** is used to illustrate the location of effects.

genotypes, consistent with their known functions. Although the *ful* genotype exhibits reduced shattering, dehiscence-related genes are expressed in the valve due to de-repression of native *SHP*. Therefore, expression of *ADPG1/2* in the *ful* background appears to reflect expression of *SHP*-repressed genes, whereas *NST3* expression is a manifestation of reduced shattering independent of *SHP*.

Similarities and differences between seed (embryo) and silique

Siliques and seeds follow distinct but coordinated developmental programs and have some similar morphogenetic and metabolic processes. For instance, both seeds and siliques desiccate during late maturation whereas siliques and endosperm senesce but embryos do not. Nutrient reserves in seeds account for 90% or more of the seed dry weight and in *Brassica* is comprised mostly of oils (triacyglycerols), and specialized SSPs.

Expression of genes coding for SSPs were highly upregulated in silique walls of *Arabidopsis* (Col-0).[31] It is not clear why there were abundant transcripts for SSPs and oil body associated proteins in valves of *Arabidopsis* and *Brassica* even in the senescing stage. Moreover, these genes were upregulated in *B. juncea* relative to *B. napus* and in *ful* vs. WT comparison. High expressions of *LEA*s and stress/senescence/drought responsive genes (e.g. *RAB18*, *DI21*, *SAG21*, *ERD14*, *LTI30*, *LTI65*, *KIN2* and *P5CS1)* in valve tissue are most likely related to cellular dehydration during drying of pods. Interestingly, LEAs related to cold stress responses such as *COR15A*, *COR15B*, and *ERD10*/*LTI45* were downregulated in *B. juncea* relative to *B. napus*.

Previous studies have shown that LEAs are capable of stabilizing labile enzymes under stress conditions (reviewed in ref. 58) and they may be required to perform this function in siliques as well as in seeds. However, this is speculative since the extent to which LEA transcripts are translated in siliques is unknown. It is interesting that the expression of known master regulators of seed development, the TFs, *ABI3*, *FUS3*, *LEC1*/*2*, that regulate the accumulation of nutrient reserves in seed were either absent or barely detectable in the valves.

Differences in gene expression between the 2 *Brassica* species are related to dehiscence

Transcriptome comparisons between *B. juncea* and *B. napus* (**Fig. 6**; **Table 6**) revealed that large numbers of differentially regulated genes function in hormone metabolism and signaling, photosynthesis, cell wall and secondary metabolism.

The timing and amount of lignin deposition differed significantly in the 2 *Brassica* species as was evident from the light micrographs (**Fig. 4**) and microarray data (**Table 4**). However, overall there was more lignification in *B. juncea* and fewer non-lignified SL cells. Despite these observations, numerous genes in the phenylpropanoid and monolignol pathways were repressed in *B. juncea* relative to *B. napus.* However, higher expression of peroxidases in *B. juncea* may be the determinant of lignin deposition. Reduced shattering in *B. juncea* may be partly due to a

combination of a smaller SL layer and increased lignin deposition. However, either an excess or a deficiency of lignin can be associated with silique dehiscence. For example, both ectopic lignification in the whole inner valve of *ful* siliques, and absence of lignification in cells adjacent to VM in plants overexpressing *FUL* rendered pods indehiscent.[18] This suggests that the amount and localization of lignin deposition determines shattering rather than its overall presence or absence.

Lignin is not the only cell wall component that may influence shattering. The tendency of middle lamellae to rupture is likely increased by pectin degradation. Our observation that pectin degradation via PGs was downregulated in *B. juncea* relative to *B. napus* and in *shp1 x shp2* vs. WT suggests an inverse relationship between shattering and pectin accumulation.

Siliques lose water prior to dehiscence and consequently suffer dehydration stress,[24] as do embryos. It is well known that ABA induces the expression of many stress responsive genes.[57] In this study, these stress responsive genes as well as ABA biosynthetic genes were induced, and ABA catabolic genes repressed in *B. juncea* relative to *B. napus*. These results suggest that *B. juncea* tissues may be better adapted to desiccation and this may be manifested in the greater resistance of vacuolated *B. juncea* cells to collapse during desiccation (**Fig. 4F, H**). Some ABA stress responsive genes were also induced in *shp1xshp2* and *alc* relative to WT (**Table S10**), suggesting a possible association of enhanced abiotic stress responses with reduced silique dehiscence.

The significance of the down regulation of many genes encoding components of photosystem (PS) I and II, and Calvin cycle in *B. juncea* vs. *B. napus*, *ful* vs. WT and *alc* vs. WT is not clear. Degradation of photosynthetic components is an expected consequence of senescence but shatter resistance is associated with reduced senescence (as summarized below). Therefore, these differences may be a result of enhanced ABA effects in shattering-deficient genotypes. ABA strongly down-regulates chlorophyll biosynthesis and photosynthesis.[57]

Auxin biosynthesis, transport and signaling were repressed in *B. juncea* relative to *B. napus*. The consistent difference in auxin responses between the 2 species may result in differences in the VM layer. It has been shown previously that auxin is involved in VM specification,[14] so the smaller size of the SL layer in *B. juncea* may be a consequence of sustained differences in auxin responses. Later in development, these consequences may include differences in lignin deposition and other cell wall constituents between *B. juncea* and *B. napus* that we have noted.

Desiccation and senescence in the silique lead to the imposition of tension on the DZ due to contraction and loss of flexibility in the valves. It has been observed previously that cell death and organ senescence related genes were induced in senescing *Arabidopsis* siliques.[31,45] Gene expression during silique dehiscence confirms the importance of senescence, wounding and defense processes.[16,31] Ethylene and JA signaling play important roles in these processes[26,49,53] and ethylene and jasmonate signaling genes were repressed in *B. juncea* relative to *B. napus*. Results presented here suggest that the onset of senescence, wounding and defense responses were delayed or reduced in the shatter resistant genotypes. Reduced senescence may contribute toward greater resistance to pod shattering in *B. juncea* because less disruptive force is imposed on the SL.

Conclusions

Pod shattering in Brassicas depends on the presence of a layer of relatively fragile SL cells that are unlignified and with weakened cell walls due to pectin degradation. These SL cells are juxtaposed with rigid, lignified VM cells (the LL) and replum cells with reinforced secondary walls. Tension between these cell layers increases as valves shrink due to desiccation and senescence until a critical point is reached at which shattering can be triggered by a mechanical impact. The size of the SL layer and cell wall metabolism, including lignin deposition, are clearly crucial determinants of shattering. In addition, we noted that ABA signaling and stress responses were upregulated whereas ethylene- and jasmonate signaling pathways and senescence related genes were downregulated in *B. juncea* vs. *B. napus*, *shp1xshp2* vs. WT and *alc* vs. WT. These relationships suggest that reduced dehiscence is associated with more pronounced adaptive response to water stress and a reduction in the degradative processes associated with senescence. The sustained effects of auxin on cell specification, cell wall formation and senescence may be a primary determinant of variations in dehiscence. We have summarized our results in a model of silique dehiscence (**Fig. 7**).

A major objective of this study was to identify genes related to pod shatter. We have developed a list of pod shatter-related genes including 124 metabolic genes and 103 TFs (**Table S8**). Gene selection was based on expression patterns of known shatter genes or a link to cell wall, organ abscission or senescence. The genes listed here may serve as starting points for the functional analysis of specific aspects of dehiscence. Study of these genes will provide a better understanding of silique dehiscence and lead to new strategies for modulating pod shattering via transgenic alteration of selected target genes. As noted earlier, shattering is increased by stresses such as heat, drought and wind, therefore reduction of shattering is a useful approach to improving performance under abiotic stress.

Materials and Methods

Plant materials and growth conditions

Arabidopsis thaliana (Col-0 ecotype) wild type (WT) and mutant (*shp1xshp2*, *ful, alc* and *ind*) plants were grown under long-day conditions at 22°C and 40% humidity with 16 h of 150 μE light and 8 h dark cycles. Seeds of T-DNA insertion mutant lines for *shp1xshp2, ful*, *alc* and *ind* were obtained from the Arabidopsis Biological Research Center (ABRC) with accession numbers respectively: SALK_CS3844, SALK_033647, SALK_103763 and SALK_010533. Homozygous plants were selected by PCR (as described in ref. 59). Siliques from homozygous plants of *shp1xshp2* and *alc* were indehiscent whereas that of *ful* was small as described previously.[4,15,17] However, *ind* siliques were dehiscent like WT indicating the possible loss of T-DNA

insert and hence were not studied further. Seeds of *B. napus* (cv. Nexera 715) and *B. juncea* (cv Vniimk405) were provided by DowAgroSciences. Growth conditions for *Brassica* plants were 22°C day and 18°C night with 16 h of 250-300 μE light and 8 h dark.

Developmental stages, tissue collection and RNA extraction

Tissue was collected from 6 developmental stages in *Arabidopsis* and *Brassica*. The stages were defined as follows: stage 1, embryos were approximately at heart stage and siliques were 70-90% elongated and 50% expanded with respect to diameter; stage 2, embryos were approximately at the bent cotyledon stage and occupied approximately 50-90% of the volume of the seed sac; stage 3, green silique color immediately prior to yellowing; stage 4, siliques were intermediate between green and yellow color; stage 5, siliques were yellow or green-yellow and stage 6, siliques were brown or yellow-brown. In a separate series of tissue collections, *Arabidopsis* flowers of WT and *ful* were tagged and green siliques were harvested at 6 and 11 days post anthesis (DPA) and green to yellow siliques were collected at 14 DPA.

In over 70% of samples, 6 independent biological replicates were collected of each tissue stage and in each replicate, tissues were harvested from no less than 10 (*Arabidopsis*) and 4 (*Brassica*) plants. DZ and valve tissues of *Brassica* were dissected under a microscope at stages 1, 2 and 4. Dissected tissues were frozen in dry ice and RNA was isolated using the RNAqueous RNA isolation kit (Ambion AM7021). Furthermore, whole siliques of *Arabidopsis* (with seeds) and *Brassica* (without seeds) were also collected in dry ice at stages 3, 5 and 6. For *Brassica* siliques (stages 3, 5 and 6), valve was peeled manually from septum-replum then frozen in liquid nitrogen and stored at −80°C until RNA was isolated (as described in ref. 60). In addition, *Arabidopsis* siliques of WT and *ful* plants were collected at 6 DPA, 11 DPA and 14 DPA in RNALater solution (Ambion AM1912) and seed, stigma, style and gynophore were removed from pods under a dissecting microscope and total RNA was isolated from these pod tissues using the RNAqueous kit as described above. The RNA quality was assessed in a Bioanalyzer (Agilent) prior to labeling and the RNA integrity numbers (RIN) obtained were in the range 7-9.

Microarray labeling, hybridization and data acquisition

Sample preparation and hybridization of Brassica and Arabidopsis samples on Arabidopsis microarrays without RNA amplification

Five micrograms of total RNA isolated from whole siliques of *Arabidopsis* and manually dissected valves of *Brassica* were used for cDNA synthesis using 3DNA Array 900 (Genisphere Inc.. cat# W500130 and W500140) and at least 6 independent hybridizations were performed for each type of sample. cDNA was labeled either with Cy3 or Cy5 followed by hybridization onto full genome Arabidopsis oligonucleotide microarray slides obtained from the University of Arizona (http://ag.arizona.edu/microarray/) and washed according to the manufacturer's instructions for 2 color hybridizations except for prehybridization. Immediately prior to use, slides were prehybridized for 20 mins at 65°C in a Coplin jar containing 3.5x SSC, 0.1% SDS and 10 mg/ml BSA. Subsequently, slides were washed for 1 min in autoclaved double distilled water (ddH_2O) and for 1 min in isopropanol and then dried using a filtered air flow. Hybridization was performed in a hybridization cassette (ArrayIt cat#AHC). Each slide was scanned for Cy3 and Cy5 emissions at a resolution of 10 μm per pixel using a GenePix 4000B scanner (Molecular Devices).

RNA amplification

For microscopically dissected tissues of *Brassica* and *Arabidopsis* WT and *ful* siliques from which seeds were removed, there was limited tissue availability and a consequent low quantity of total RNA. In addition, Combimatrix slide chemistry is incompatible with the 3DNA Array 900 system. Therefore an aRNA amplification system (Allyl MessageAmp II aRNA amplification kit from Ambion: cat#AM1753) was adopted and 800 ng total RNA was used as a starting material to make fluorescent dye labeled aRNA.

Hybridization of Brassica samples to Combimatrix Brassica microarrays

For quantifying *Brassica* gene expression, we used custom-built Combimatrix 90k Brassica arrays. Array probes were developed using public EST sequences obtained from *Brassica* tissues.[28] These ESTs were assembled into 95,000 unigenes. Unique 35-mer probe sequences were designed and synthesized *in situ* on slides using the Combimatrix technology (Combi Matrix diagnostics). Each full length individual *Brassica* contig/singleton was aligned against the *A. thaliana* unigene (TAIR8 cds database) and Uniprot plant sequence database and was scored by the BLAST similarity matrices. Combimatrix slide chemistry has inherent fluorescence at lower wavelengths; therefore, only Cy5 dye labeling and hence single color analyses were performed. Furthermore, as Combimatrix slides are not suitable for the autoPMT function in the GenePix scanner, 10 alien RNA spikes (Stratagene cat#252561-252570) were added to the 800 ng total RNA. Five micrograms of Cy5 labeled aRNA were fragmented using reagents from Ambion (cat#AM8740) prior to the hybridization step. Although aRNA amplification routinely produces around 60 μg aRNA from 800 ng total RNA, separate aRNA preparations were made for all hybridizations and at least 6 independent hybridizations were performed for each type of sample.

Combimatrix slide hybridization, washing, scanning and post scan stripping of labeled probes from slides and rehybridization were performed according to the manufacturer's instructions (CustomArray™ 90K microarray; protocol#PTL020). GenePix scanner settings for Combimatrix slides were 5 μM pixel size and 130 μM focus position. During scanning, the spot intensity value of each RNA spike was kept approximately the same for all hybridized slides.

Hybridization of Arabidopsis samples to Arabidopsis microarrays using amplified RNA.

For 2 color hybridizations on *Arabidopsis* arrays (consisting of *ful* vs. WT comparisons with seeds removed), 4 independent hybridizations were performed and the above aRNA protocol was modified slightly as follows: No RNA spikes were added to the 800 ng starting total RNA and each aRNA prep was labeled with either Alexa647 or Alexa555 dyes. Slides were UV cross-linked and prehybridized as described above. Five micrograms of each Alexa647 and Alexa555 labeled aRNA were mixed together, fragmented and then added to 68 μl hybridization solution (SlideHyb #1 buffer; Ambion cat#AM8861). A 25X60 LifterSlip (Erie Scientific Company cat#25x60I-2-4789) was placed on top of the arrayed area and around 80 μl of the above labeled aRNA and hybridization solution mixture was added at one edge of the LifterSlip and the slide was placed inside an ArrayIt hybridization cassette. Hybridization was performed at 45°C overnight with gentle horizontal agitation at 40 rpm. After hybridization, the LifterSlip was removed in 2xSSC and 0.2% SDS solution prewarmed at 45°C. Slide washing was carried out with gentle agitation of 40 rpm as follows: 1) 10 min washing in 2xSSC and 0.2% SDS solution prewarmed at 45°C; 2) 10 min in 2xSSC at room temperature (RT) and 3) 10 min in 0.2xSSC at RT. Slides were scanned by a GenePix scanner.

Initial data extraction

Calculation of the signal intensity of spots and flagging of bad spots were carried out in GenePix Pro 6.1 software (Molecular Devices).

Quality control of data for subsequent analysis

All primary data, including images were uploaded into BioArray Software Environment (BASE) where background signal subtraction was performed.[61] Subsequently, normalization (Print-tip loess), filtering bad spots and control spots and filtering minimum channel intensity (intensity for both channel should be <300 in most cases) were also carried out. Then calculation of correlation coefficients between replicates and visual spot quality inspection was also performed in BASE. Afterward, data were transferred to GeneSpring GX 10.0.2 (Agilent) for higher order data analysis. Single color Combimatrix microarray data was uploaded directly from GenePix Pro 6.1 into GeneSpring where the default normalization (each measurement was divided by the 75th percentile of all measurements in that sample and each gene intensity was divided by the median of its measurements in all samples), filtering of flagged spots and calculation of correlation coefficient among replicates were performed. For both 2 and single color hybridizations, quality control on sample data was performed in GeneSpring.

Determining differentially expressed genes and enrichment of biological pathways

A t-test against zero together with Benjamini-Hotchberg multiple testing correction with a 0.05 p-value cut-off was performed in GeneSpring to obtain statistically differentially expressed gene sets. Furthermore, a fold change ≥2.0 and ≥4.0, for 2 color and single color platforms, respectively, were employed as additional criteria of biological significance. Due to the large number of changes in expression, a conservative approach of 4-fold change was taken to reduce *Brassica* false positives. Afterward, log2 expression values were uploaded into MapMan ImageAnnotator version 3.0.0RC3[44] for pathway analysis. Microarray data from multiple contigs (probes) for the same gene were averaged before uploading to MapMan. To obtain statistically significant enriched biological pathways, a Wilcoxon rank sum t-test embedded in MapMan was performed with a p-value cut-off 0.05 and Benjamini Hochberg multiple testing correction. The heat map was generated using heatmap builder version 1.1 software.[62] For multiple comparisons, 1-way ANOVA was performed in GeneSpring to obtain statistically differentially expressed gene lists. Additional quality control on gene lists for false positive / negative was performed in BASE using its spot visualization feature. Only genes that were differentially expressed in more than one comparison are reported.

Light microscopy

Canola siliques at various developmental stages were cut transversely by hand with a Teflon-coated razor blade under 3% (v/v) glutaraldehyde in 0.05 M PIPES buffer (pH 7.4) into thin 'coins' on a sheet of dental wax, then transferred to a scintillation vial containing this fixative for 2 h at room temperature with vacuum applied several times to remove air from the tissue. The specimens were then washed twice (15 min each) in cold PIPES buffer and dehydrated in an ethanol series of 25, 50 and 75% at 4°C, 2 hours each step, then 100% ethanol at −20°C for 24 hours. Samples were then infiltrated with increasing concentrations of LR White resin (25, 50, 75, and 100%) at −20°C for 24 h each step. The specimens were then placed on a rotator at room temperature for 24 hours and subsequently transferred individually to flat-bottomed BEEM capsules and polymerized at 55°C for 2 h. Sections for light microscopic examination were cut 0.5 μm thick on an ultramicrotome with a diamond knife, collected on slides, dried on a hotplate, and stained for 10–30 seconds with 1% (w/v) toluidine blue in 1% (w/v) sodium borate. Sections were then mounted with Polymount (Polysciences), observed on a Leica DM5000 microscope, and recorded with a Leica DCF500 digital camera.

Disclosure of Potential Conflicts of Interest

No potential conflicts of interest were disclosed.

Acknowledgments

The authors would like to thank Mr. Chad Matsalla for assistance with Bioinformatics, Dr. Van Ripley of Dow AgroSciences for providing *B. juncea* seeds, and Dr. Mark Thomson, Dr. Allan Feurtado and Dr. Daiqing Huang for helpful discussions. Dr. Yuejin Sun provided helpful input into microarray experiments and Dr. Tom Skokut provided valuable contributions during project initiation.

Funding

This project was funded by the National Research Council of Canada and Dow AgroSciences. This paper is NRCC number 55577.

Supplemental Material

Supplemental data for this article can be accessed on the publisher's website.

References

1. MacLeod J. Oilseed rape. Cambridge: Cambridge Agricultural, 1981; 107-19.
2. Kadkol GP, Macmillan RH, Burrow RP, Halloran GM. Evaluation of *Brassica* genotypes for resistance to shatter. I. Development of a laboratory test. Euphytica 1984; 33:63-73.
3. Child RD, Summers JE, Babij J, Farrent JW, Bruce DM. Increased resistance to pod shatter is associated with changes in the vascular structure in pods of a resynthesized *Brassica napus* line. J Exp Bot 2003; 54:1919-30; PMID:12837816
4. Liljegren SJ, Ditta GS, Eshed Y, Savidge B, Bowman JL, Yanofsky MF. *SHATTERPROOF* MADS-box genes control seed dispersal in *Arabidopsis*. Nature 2000; 404:766-70; PMID:10783890
5. Liljegren SJ, Roeder AHK, Kempin SA, Gremski K, Østergaard L, Guimil S, Reyes DK, Yanofsky MF. Control of fruit patterning in *Arabidopsis* by *INDEHISCENT*. Cell 2004; 116:843-53; PMID:15035986
6. Østergaard L, Kempin SA, Bies D, Klee HJ, Yanofsky MF. Pod shatter-resistant *Brassica* fruit produced by ectopic expression of the *FRUITFULL* gene. Plant Biotech J 2006; 4:45-51.
7. Mitsuda N, Ohme-Takagi M. NAC transcription factors NST1 and NST3 regulate pod shattering in a partially redundant manner by promoting secondary wall formation after the establishment of tissue identity. Plant J 2008; 56:768-78; PMID:18657234; http://dx.doi.org/10.1111/j.1365-313X.2008.03633.x
8. Ogawa M, Kay P, Wilson S, Swain SM. ARABIDOPSIS DEHISCENCE ZONE POLYGALACTURONASE1 (ADPG1), ADPG2, and QUARTET2 are polygalacturonases required for cell separation during reproductive development in *Arabidopsis*. Plant Cell 2009; 21:216-33; PMID:19168715; http://dx.doi.org/10.1105/tpc.108.063768
9. Lewis MW, Leslie ME, Liljegren SJ. Plant separation: 50 ways to leave your mother. Curr Opin Plant Biol 2006; 9:59-65; PMID:16337172
10. Girin T, Sorefan K, Østergaard L. Meristematic sculpting in fruit development. J Exp Bot 2009; 60:1493-502; PMID:19246597; http://dx.doi.org/10.1093/jxb/erp031
11. Peterson M, Sander L, Child R, van Onckelen H, Ulvskov P, Borkhardt B. Isolation and characterization of a pod dehiscence zone-specific polygalacturonase from *Brassica napus*. Plant Mol Biol 1996; 31:517-27; PMID:8790285
12. Dinneny JR, Weigel D, Yanofsky MF. A genetic framework for fruit patterning in *Arabidopsis thaliana*. Development 2005; 132:4687-96; PMID:16192305
13. Roeder AH, Yanofsky MF. Fruit development in *Arabidopsis*. Arabidopsis Book. Rockville, MD. 2006; 4: e0075. http://dx.doi.org/10.1199/tab.0075
14. Sorefan K, Girin T, Liljegren SJ, Ljung K, Robles P, Galvan-Ampudia CS, Offringa R, Friml J, Yanofsky MF, Østergaard L. A regulated auxin minimum is required for seed dispersal in *Arabidopsis*. Nature 2009; 459:583-6; PMID:19478783; http://dx.doi.org/10.1038/nature07875
15. Rajani S, Sundaresan V. The *Arabidopsis* myc/bHLH gene *ALCATRAZ* enables cell separation in fruit dehiscence. Curr Biol 2001; 11:1914-22; PMID:11747817
16. Spence J, Vercher Y, Gates P, Harris N. 'Pod shatter' in *Arabidopsis thaliana*, *Brassica napus* and *B. juncea*. J Microsc 1996; 181:195-203.
17. Gu Q, Ferrándiz C, Yanofsky MF, Martienssen R. The *FRUITFULL* MADS-box gene mediates cell differentiation during *Arabidopsis* fruit development. Development 1998; 125:1509-17; PMID:9502732
18. Ferrándiz C, Liljegren SJ, Yanofsky MF. Negative regulation of the *SHATTERPROOF* genes by *FRUITFULL* during *Arabidopsis* fruit development. Science 2000; 289:436-8; PMID:10903201
19. Meakin PJ, Roberts JA. Dehiscence of fruit in oilseed rape (*Brassica napus* L.): II. The role of cell wall degrading enzymes and ethylene. J Exp Bot 1990; 41:1003-11.
20. Meakin PJ, Roberts JA. Anatomical and biochemical changes associated with the induction of oilseed rape (*Brassica napus*) pod dehiscence by *Dasineura brassicae* (Winn.). Ann Bot 1991; 67:193-7.
21. Bonghi ZC, Casadoro G, Ramina A, Rascio N. Abscission in leaf and fruit explants of *Prunus persica* (L.) Batsch. New Phytol 1993; 123:555-65.
22. Cho H-T, Cosgrove DJ. Altered expression of expansin modulates leaf growth and pedicel abscission in *Arabidopsis thaliana*. Proc Natl Acad Sci USA 2000; 97:9783-8; PMID:10931949
23. Sander L, Child R, Ulvskov P, Albrechtsen M, Borkhardt B. Analysis of a dehiscence zone endo-polygalacturonase in oilseed rape (*Brassica napus*) and *Arabidopsis thaliana*: evidence for roles in cell separation in dehiscence and abscission zones, and in stylar tissues during pollen tube growth. Plant Mol Biol 2001; 46:469-79; PMID:11485203
24. Squires TM, Gruwel MLH, Zhou R, Sokhansanj S, Abrams SR, Cutler AJ. Dehydration and dehiscence in siliques of *Brassica napus* and *Brassica rapa*. Can J Bot 2003; 81:248-54.
25. Arnaud N, Girin T, Sorefan K, Fuentes S, Wood TA, Lawrenson T, Sablowski R, Østergaard L. Gibberellins control fruit patterning in *Arabidopsis thaliana*. Genes Dev 2010; 24:2127-32; PMID:20889713; http://dx.doi.org/10.1101/gad.593410
26. Child R, Chauvaux N, John K, Ulvskov P, van Onckelen H. Ethylene biosynthesis in oilseed rape pods in relation to pod shatter. J Exp Bot 1998; 49:829-38.
26. Ferrándiz C. Regulation of fruit dehiscence in *Arabidopsis*. J Exp Bot 2002; 53:2031-8; PMID:12324527
27. Johnson-Flanagan AM, Spencer MS. Ethylene production during development of mustard (*Brassica juncea*) and canola (*Brassica napus*) seed. Plant Physiol 1994; 106:601-6; PMID:12232353
28. Huang D, Koh C, Feurtado JA, Tsang E, Cutler AJ. MicroRNAs and their putative targets in *Brassica napus* seed maturation. BMC Genomics 2013; 14:140-64; PMID:23448243; http://dx.doi.org/10.1186/1471-2164-14-140
29. Fei H, Ferhatoglu Y, Tsang E, Huang D, Cutler AJ. Metabolic and hormonal processes associated with the induction of secondary dormancy in *Brassica napus* seeds. Botany 2009; 87:585-96.
30. Ruuska SA, Girke T, Benning C, Ohlrogge JB. Contrapuntal networks of gene expression during *Arabidopsis* seed filling. Plant Cell 2002; 14:1191-206; PMID:12084821
31. Carol W, Thomas JWY, Anthony DS, Vicky B-W, Jeremy AR. A molecular and structural characterization of senescing Arabidopsis siliques and comparison of transcriptional profiles with senescing petals and leaves. Plant J 2009; 57:690-705; PMID:18980641; http://dx.doi.org/10.1111/j.1365-313X.2008.03722.x
32. Baud S, Dubreucq B, Miquel M, Rochat C, Lepiniec L. Storage reserve accumulation in Arabidopsis: metabolic and developmental control of seed filling. The Arabidosis Book. Rockville, MD. 2008; 6:e0113; PMID:22303238; http://dx.doi.org/10.1199/tab.0113.
33. Roeder AHK, Ferrándiz C, Yanofsky MF. The role of the REPLUMLESS homeodomain protein in patterning the *Arabidopsis* fruit. Curr Biol 2003; 13:1630-5; PMID:13678595
34. <!——> Pérez-Rodríguez P, Riaño-Pachón DM, Corrêa LGG, Rensing SA, Kersten B, Mueller-Roeber B. PlnTFDB: updated content and new features of the plant transcription factor database. Nucl Acids Res 2010; 38:D822-7.
35. Herrmann KM, Weaver LM. The shikimate pathway. Annu Rev Plant Physiol Plant Mol Biol 1999; 50:473-503; PMID:15012217
36. Ruegger M, Meyer K, Cusumano JC, Chapple C. Regulation of ferulate-5-hydroxylase expression in *Arabidopsis* in the context of sinapate ester biosynthesis. Plant Physiol 1999; 119:101-10; PMID:9880351
37. Boerjan W, Ralph J, Baucher M. Lignin biosynthesis. Annu Rev of Plant Biol 2003; 54:519-46.
38. Caffall KH, Mohnen D. The structure, function, and biosynthesis of plant cell wall pectic polysaccharides. Carbohydr Res 2009; 344:1879-900; PMID:19616198; http://dx.doi.org/10.1016/j.carres.2009.05.021
39. Benen JAE, Kester HCM, Visser J. Kinetic characterization of *Aspergillus niger* N400 endopolygalacturonases I, II and C. Eur J Biochem 1999; 259:577-85; PMID:10092840
40. Stolle-Smits T, Beekhuizen JG, Kok MTC, Pijnenburg M, Recourt K, Derksen J, Voragen AGJ. Changes in cell wall polysaccharides of green bean pods during development. Plant Physiol 1999; 121:363-72; PMID:10517827
41. Ridley BL, O'Neill MA, Mohnen D. Pectins: structure, biosynthesis, and oligogalacturonide-related signaling. Phytochemistry 2001; 57:929-67; PMID:11423142
42. Ferrari S, Vairo D, Ausubel FM, Cervone F, De Lorenzo G. Tandemly duplicated Arabidopsis genes that encode polygalacturonase-inhibiting proteins are regulated coordinately by different signal transduction pathways in response to fungal infection. Plant Cell 2003; 15:93-106; PMID:12509524
43. Rose JKC, Braam J, Fry SC, Nishitani K. The XTH family of enzymes involved in xyloglucan endotransglucosylation and endohydrolysis: current perspectives and a new unifying nomenclature. Plant Cell Physiol 2002; 43:1421-35; PMID:12514239
44. Thimm O, Bläsing O, Gibon Y, Nagel A, Meyer S, Krüger P, Selbig J, Müller LA, Rhee SY, Stitt M. MAPMAN: a user-driven tool to display genomics data sets onto diagrams of metabolic pathways and other biological processes. Plant J 2004; 37:914-39; PMID: 14996223
45. Buchanan-Wollaston V, Page T, Harrison E, Breeze E, Lim PO, Nam HG, Lin JF, Wu SH, Swidzinski J, Ishizaki K, et al. Comparative transcriptome analysis reveals significant differences in gene expression and signalling pathways between developmental and dark/starvation-induced senescence in Arabidopsis. Plant J 2005; 42:567-85; PMID:15860015
46. Jackson RG, Lim EK, Li Y, Kowalczyk M, Sandberg G, Hoggett J, Ashford DA, Bowles DJ. Identification and biochemical characterization of an *Arabidopsis* indole-3-acetic acid glucosyltransferase. J Biol Chem 2001; 276:4350-6; PMID:11042207
47. Leyser O. Dynamic integration of auxin transport and signalling. Curr Biol 2006; 16:R424-33; PMID:16753558
48. Staswick PE, Serban B, Rowe M, Tiryaki I, Maldonado MT, Maldonado MC, Suza W. Characterization of an Arabidopsis enzyme family that conjugates amino acids to indole-3-acetic acid. Plant Cell 2005; 17:616-27; PMID:15659623
49. Binder BM, Walker JM, Gagne JM, Emborg TJ, Hemmann G, Bleecker AB, Vierstra RD. The *Arabidopsis* EIN3 binding F-box proteins EBF1 and EBF2 have

distinct but overlapping roles in ethylene signaling. Plant Cell 2007; 19:509-23; PMID:17307926
50. Wang KLC, Yoshida H, Lurin C, Ecker JR. Regulation of ethylene gas biosynthesis by the *Arabidopsis* ETO1 protein. Nature 2004; 428:945-950.
51. Rzewuski G, Sauter M. Ethylene biosynthesis and signaling in rice. Plant Sci 2007; 175:32-42.
52. Chico JM, Chini A, Fonseca S, Solano R. JAZ repressors set the rhythm in jasmonate signaling. Curr Opin Plant Biol 2008; 11:486-94; PMID:18653378; http://dx.doi.org/10.1016/j.pbi.2008.06.003
53. Browse J. The power of mutants for investigating jasmonate biosynthesis and signaling. Phytochemistry 2009; 70:1539-46; PMID:19740496; http://dx.doi.org/10.1016/j.phytochem.2009.08.004
54. Nambara E, Marion-Poll A. Abscisic acid biosynthesis and catabolism. Annu Rev Plant Biol 2005; 56:165-85; PMID:15862093
55. Zou J, Abrams GD, Barton DL, Taylor DC, Pomeroy MK, Abrams SR. Induction of lipid and oleosin biosynthesis by (+)-abscisic acid and its metabolites in microspore-derived embryos of *Brassica napus* L.cv Reston. Biological responses in the presence of 8'-hydroxyabscisic acid. Plant Physiol 1995; 108:563-71; PMID:12228493
56. Jiang L, Abrams SR, Kermode AR. Vicilin and napin storage-protein gene promoters are responsive to abscisic acid in developing transgenic tobacco seed but lose sensitivity following premature desiccation. Plant Physiol 1996; 110:1135-44; PMID:12226247
57. Huang D, Jaradat MR, Wu W, Ambrose SJ, Ross AR, Abrams SR, Cutler AJ. Structural analogs of ABA reveal novel features of ABA perception and signaling in Arabidopsis. Plant J 2007; 50:414-28; PMID:17376162
58. Hundertmark M, Hincha D. LEA (Late Embryogenesis Abundant) proteins and their encoding genes in *Arabidopsis thaliana*. BMC Genomics 2008; 9:118-39; PMID:18318901; http://dx.doi.org/10.1186/1471-2164-9-118
59. Alonso JM, Stepanova AN, Leisse TJ, Kim CJ, Chen H, Shinn P, Stevenson DK, Zimmerman J, Barajas P, Cheuk R, et al. Genome-wide insertional mutagenesis of *Arabidopsis thaliana*. Science 2003; 301:653-7; PMID:12893945
60. Suzuki Y, Kawazu T, Koyama H. RNA isolation from siliques, dry seeds, and other tissues of *Arabidopsis thaliana*. Biotechniques 2004; 37:542-4; PMID:15517963
61. Saal LH, Troein C, Vallon-Christersson J, Gruvberger S, Borg A, Peterson C. BioArray Software Environment (BASE): a platform for comprehensive management and analysis of microarray data. Genome Biol 2002; 3:software0003.1-software0003.6; PMID:12186655
62. King JY, Ferrara R, Tabibiazar R, Spin JM, Chen MM, Kuchinsky A, Vailaya A, Kincaid R, Tsalenko A, Deng DX, et al. Pathway analysis of coronary atherosclerosis. Physiol Genomics 2005; 23:103-18; PMID:15942018